An improved stress map for Italy and surrounding regions (central Mediterranean)

Paola Montone, M. Teresa Mariucci, Silvia Pondrelli, and Alessandro Amato
Istituto Nazionale di Geofisica e Vulcanologia, Rome, Italy

Received 24 July 2003; revised 6 May 2004; accepted 24 June 2004; published 21 October 2004.

[1] We present an updated present-day stress data compilation for the Italian region and discuss it with respect to the geodynamic setting and the seismicity of the area. We collected and analyzed 190 new stress data from borehole breakouts, seismicity, and active faults and checked in detail the previous compilation [*Montone et al.*, 1999]. Our improved data set consists of 542 data, 362 of which with a reliable quality for stress maps. The Italian region is well sampled, allowing the computation of constrained smoothed stress maps; for surrounding regions we added the World Stress Map 2003 release data. These maps depict the active stress conditions and, in the areas where the data are sparse, contribute to understand the relationship between active stress, past tectonic setting, and the seismicity of the study region. The new data are particularly representative along the northern Apennine front, from the Po Plain to offshore the Adriatic, and along the southern Tyrrhenian Sea, north of Sicily, where they point out a compressive tectonic regime. In the Alps both compressive and transcurrent regimes are observed. Our data also confirm that the whole Apenninic belt and the Calabrian arc are extending. Along the central Adriatic coast, changes from one stress regime to another are shown by abrupt variations in the minimum horizontal stress directions. Other gentler stress rotations, as, for instance, from the southern Apennines to the Calabrian arc or along the northern Apennines, follow the curvature of the arcs and are not associated to a stress regime variation. *INDEX TERMS:* 7230 Seismology: Seismicity and seismotectonics; 8164 Tectonophysics: Stresses—crust and lithosphere; 9335 Information Related to Geographic Region: Europe;
KEYWORDS: active stress, earthquakes, borehole breakouts, Italy

Citation: Montone, P., M. T. Mariucci, S. Pondrelli, and A. Amato (2004), An improved stress map for Italy and surrounding regions (central Mediterranean), *J. Geophys. Res.*, *109*, B10410, doi:10.1029/2003JB002703.

1. Introduction

[2] The geodynamic setting of the Italian region is particularly complex. This area is involved in the N-S convergence of Africa and Eurasian plates, but is presently undergoing NE-SW extension perpendicular to the Apenninic fold and thrust belt [*Anderson and Jackson*, 1987; *Westaway*, 1992; *Pondrelli et al.*, 1995; *Amato and Montone*, 1997], approximately coeval with the opening of the Tyrrhenian basin which started in Late Tortonian times [*Patacca and Scandone*, 1989]. This process acted in the presence of a subduction system extending from Sicily to northern Apennines as shown by tomographic images, where the Adriatic plate is still present as a nearly continuous lithospheric body below the Apennines [*Lucente et al.*, 1999; *Amato and Cimini*, 2001; *Piromallo and Morelli*, 2003]. This subduction is still active in the southern Tyrrhenian Sea, where seismicity is located down to 600 km of depth [*Selvaggi*, 2001], and probably beneath the northern Apennines, where earthquakes down to 90 km of depth have been recorded [*Selvaggi and Amato*, 1992].

0148-0227/04/2003JB002703$09.00

[3] All these complexities should be reflected also in the stress field distribution, whose definition may contribute to the understanding of involved driving forces and their modeling. The World Stress Map first issue [*Zoback*, 1992] was rather poor for the Italian region and we developed our preceding compilation to enrich it [*Montone et al.*, 1999].

[4] We now present additional data concerning the active stress field in Italy, obtained from borehole breakouts in deep wells (Figure 1), earthquake data (Figure 2) and fault measurements. With respect to *Montone et al.* [1999], this data set has been increased by about 50%: from 352 entries we have today 542 data, including all qualities (from A, the best, to E, discarded data). In detail, we have now 329 borehole breakouts (149 of which with A, B or C quality), 186 earthquake fault plane solutions (with B or C quality, $M \geq 4.0$), 20 formal inversions of earthquake focal mechanisms (B quality, except one data) and 7 fault data with C quality. In terms of reliable stress indicators percentage, our data set is now characterized by 61% of borehole breakouts, 34% of earthquake data, 4% of focal mechanism inversions and finally 1% of fault data.

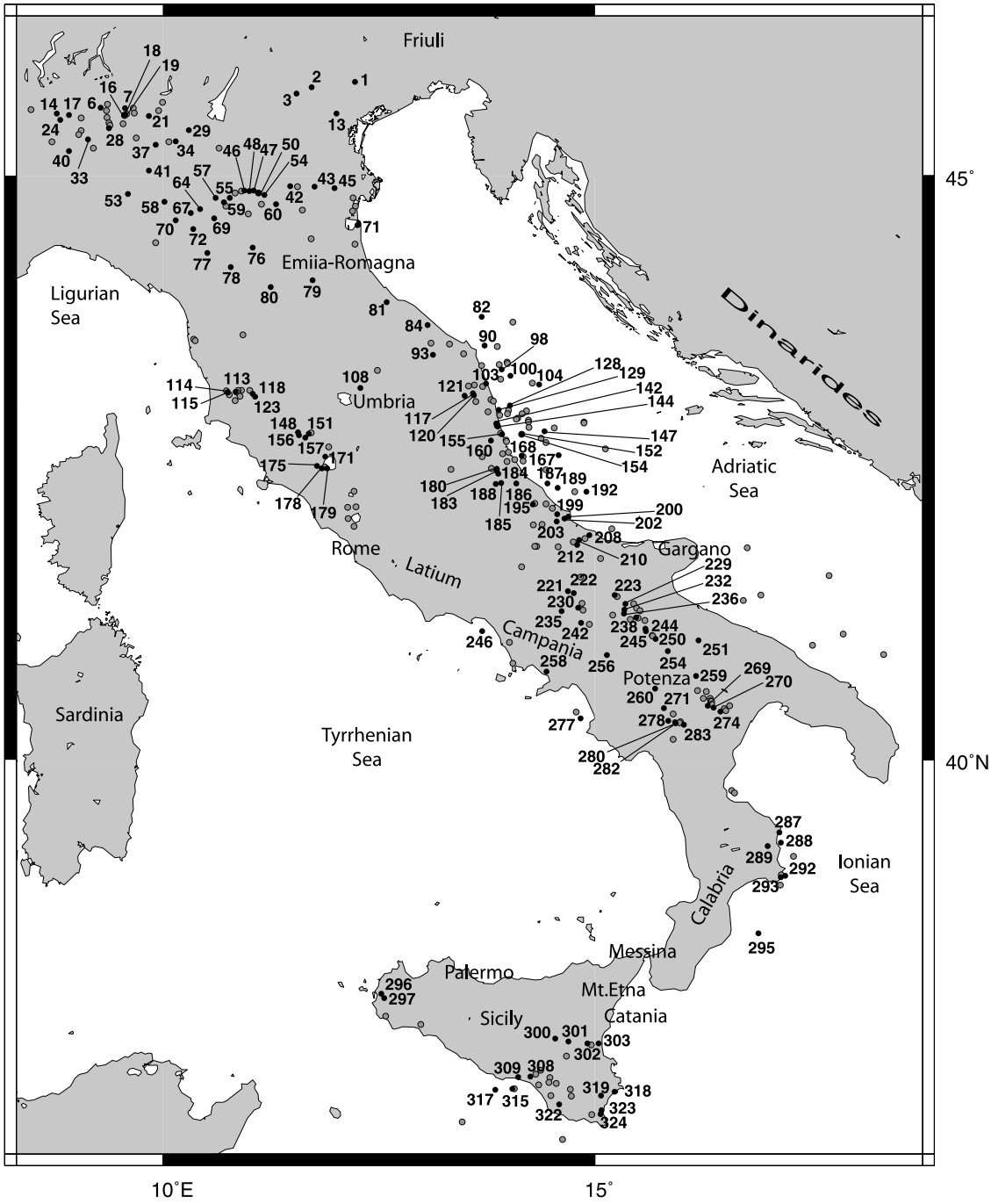

Figure 1. Location map of analyzed wells. Black dots are for breakout ranked with quality A, B and C; grey dots are for data with quality D and E. Numbers correspond to data set of Table 1.

[5] This data set is presently the most updated, complete and reviewed catalogue of active stress indicators for Italy and is used to compute smoothed stress orientation maps useful to determine reliable stress directions also where data are sparse. The only previous interpolated map of stress in the Mediterranean region was done by *Rebaï et al.* [1992], where only a small number of data was available for Italy. In the second part of this paper, after the description of the new data, we present a smoothed stress map of Italy and adjacent regions that better defines variations in stress direction and regime. Moreover, we compare it with other data set in order to discuss the active stress field with respect to the expected future seismicity of the area.

2. Data Presentation

[6] In this paragraph we describe only the new data included in our data set; we do not make any mention to the different methods and techniques used to determine them, for which we refer to the wide bibliography reported by *Zoback* [1992] and *Montone et al.* [1999] as concerns the Italian data set. We also refer the reader to *Bell and Gough*

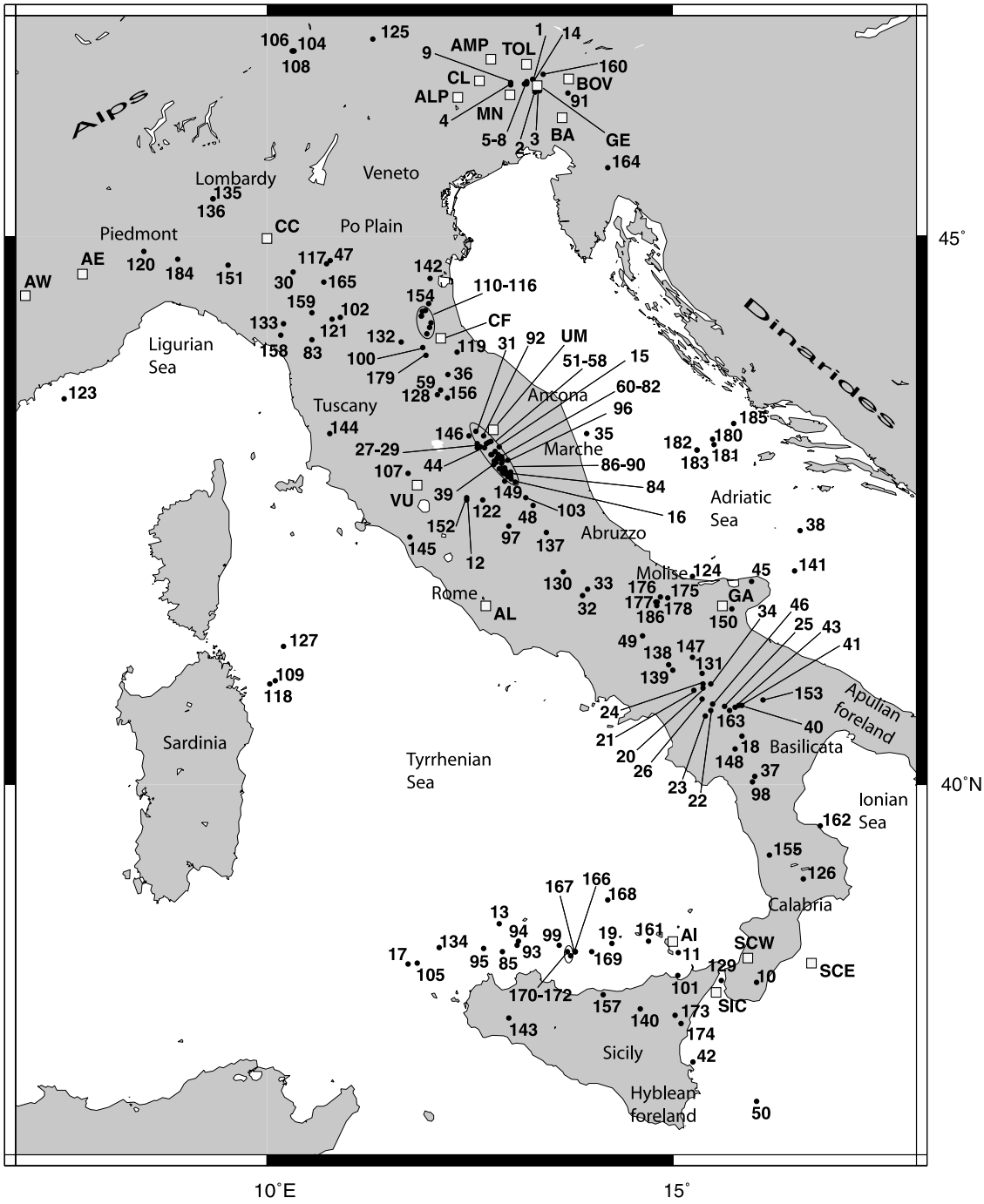

Figure 2. Location map of seismicity data. Black dots are single seismic events (numbers correspond to data set of Table 2). White squares with labels are formal inversions of stress axes reported in Table 3.

[1983] for the borehole breakout analysis from four-arm caliper records, to *Dziewonski et al.* [1981, 1983] for centroid moment tensor (CMT) computation, to *Arvidsson and Ekström* [1998] for regional centroid moment tensor (RCMT) computation, to *Frepoli and Amato* [1997] for earthquake stress inversion data and to *Angelier* [1984] for fault data. We assigned a quality value to each datum, from A (the best) to E (discarded), as proposed by *Zoback* [1992] for the World Stress Map. Applying this standard quality ranking makes our data set easily available for the World Stress Map or other studies where these data are needed and allows the comparison of very different types of information.

[7] Moreover, for the assumptions concerning the selection of the data, we refer to those previously described by several authors [e.g., *Zoback*, 1992, and references therein; *Anderson*, 1951; *McGarr and Gay*, 1978]. In this paper we report the results in terms of minimum horizontal stress orientations ($S_{h\min}$, corresponding to either σ_2 or σ_3, with $\sigma_1 > \sigma_2 > \sigma_3$), both for the stress map of Italy and for the smoothed maps.

[8] Following *Montone et al.* [1999], in this paper we also take into account mostly borehole breakouts and focal mechanisms of earthquakes. Moreover, we report a few active fault data determined from paleoseismological

Table 1. Borehole Breakout Data Set[a]

Event	Latitude, °N	Longitude, °E	S_{hmin}	SD	Q	Source
1	45.77	12.22	56	15°	B	11
2	45.73	11.72	84	5°	B	11
3	45.67	11.55	87	18°	B	11
4	45.60	9.99	5	27°	E	14
5	45.59	9.35	5	22°	D	14
6	45.56	9.73	26	21°	C	14
7	45.56	9.56	12	14°	B	14
8	45.55	9.66	85	37°	D	14
9	45.54	8.47	72	27°	D	14
10	45.54	9.95	149	38°	E	14
11	45.53	9.35	42	32°	D	14
12	45.56	9.54	169	35°	D	14
13	45.51	12.01	161	13°	C	11
14	45.51	8.77	131	11°	B	14
15	45.51	9.57	98	38°	E	14
16	45.50	9.56	79	18°	B	14
17	45.50	8.91	114	23°	C	14
18	45.50	9.55	84	13°	A	14
19	45.50	9.55	59	10°	B	14
20	45.50	9.55	99	27°	D	14
21	45.49	9.83	116	16°	C	14
22	45.48	9.35	120	37°	D	14
23	45.48	9.05	74	32°	D	14
24	45.46	8.81	140	23°	C	14
25	45.44	9.37	156	35°	E	14
26	45.43	9.53	81	33°	D	14
27	45.42	9.38	93	33°	D	14
28	45.39	9.38	123	16°	C	14
29	45.38	10.30	112	20°	B	14
30	45.37	9.05			E	14
31	45.34	9.02	23	26°	D	14
32	45.31	9.69	21	29°	E	14
33	45.30	9.13	51	26°	C	14
34	45.28	10.15	111	7°	A	14
35	45.28	10.07	4	19°	E	14
36	45.28	8.71			E	14
37	45.26	9.91	126	12°	B	14
38	45.23	9.19	83	36°	D	14
39	45.23	10.65	32	28°	D	14
40	45.21	8.91	24	23°	C	14
41	45.04	9.83	100	24°	C	11
42	44.92	11.47	119	5°	A	11
43	44.91	11.75	8	24°	C	11
44	44.91	11.56			E	11
45	44.90	11.99	27	25°	C	11
46	44.88	10.94	76	20°	B	8, 10
47	44.88	11.05	110	20°	B	8, 10
48	44.88	11.00	105	9°	A	11
49	44.88	10.91	124	26°	D	8
50	44.86	11.10	9	28°	C	11
51	44.86	11.10	12	29°	D	11
52	44.86	10.84	76	24°	D	8
53	44.86	9.60	168	22°	C	11
54	44.84	11.17	108	23°	C	8, 10
55	44.82	10.77	95	10°	B	8, 10
56	44.82	12.20	159	31°	D	11
57	44.82	10.61	127	15°	B	8, 10
58	44.79	10.02	34	19°	B	11
59	44.79	10.70	109	14°	B	8, 10
60	44.77	11.31	57	10°	B	8, 10
61	44.77	11.14			E	8
62	44.75	12.23	154	35°	D	11
63	44.75	10.73	167	7°	D	8
64	44.73	10.43	97	10°	B	8, 10
65	44.72	11.61			E	11
66	44.71	12.20	139	26°	D	11
67	44.70	10.32	62	16°	B	11
68	44.69	10.99	84	19°	D	11
69	44.65	10.59	172	11°	B	11
70	44.64	10.15	95	8°	C	11
71	44.60	12.25	100	21°	C	11
72	44.56	10.35	107	20°	C	11
73	44.48	11.71	116	30°	D	11

Table 1. (continued)

Event	Latitude, °N	Longitude, °E	S_{hmin}	SD	Q	Source
74	44.45	9.92			E	15
75	44.44	12.22			E	11
76	44.41	11.04	81	17°	C	11
77	44.37	10.51	175	14°	B	11
78	44.25	10.78	58	20°	C	11
79	44.14	11.73	129	8°	B	1, 7, 10
80	44.08	11.25	17	13°	B	15
81	43.95	12.59	160	8°	B	11
82	43.83	13.69	122	23°	C	10
83	43.79	14.05			E	15
84	43.76	13.06	156	31°	C	6, 7, 10
85	43.68	10.93			E	15
86	43.65	10.35			E	15
87	43.63	10.37			E	15
88	43.61	13.10			E	15
89	43.60	13.32			E	6, 7
90	43.59	13.72	142	21°	C	6, 7, 10
91	43.58	13.87			E	6, 7
92	43.52	13.48			E	6, 7
93	43.51	13.13	74	13°	C	10
94	43.45	13.98	175	9°	D	15
95	43.44	13.99	174	18°	D	15
96	43.43	13.89	157	15°	D	15
97	43.42	13.69	136	29°	D	15
98	43.39	13.92	122	8°	B	6, 7, 10
99	43.38	12.49	11	29°	D	6, 7
100	43.33	14.02	80	20°	C	6, 7, 10
101	43.31	13.91	120	30°	D	6, 7
102	43.27	14.28			E	6, 7
103	43.27	13.74	139	20°	C	10
104	43.26	14.36	144	24°	C	6, 7, 10
105	43.26	13.61			E	15
106	43.25	13.54	36	12°	D	15
107	43.25	13.70	127	15°	D	15
108	43.23	12.28	77	23°	C	6, 7, 10
109	43.21	11.01	143	5°	D	15
110	43.21	10.91			E	15
111	43.21	10.87			E	15
112	43.21	10.73	123	23°	D	15
113	43.20	10.84	22	22°	C	10
114	43.20	10.75	117	19°	C	10
115	43.20	10.75	27	11°	C	10
116	43.20	10.86			E	15
117	43.19	13.59	152	20°	C	10
118	43.18	11.04	89	16°	B	10
119	43.18	10.76			E	15
120	43.17	13.60	129	23°	C	6, 7, 10
121	43.17	13.49	75	25°	C	6, 7, 10
122	43.16	10.89	33	24°	D	15
123	43.16	11.06	76	21°	C	10
124	43.13	13.80	120	28°	D	6, 7
125	43.12	10.83			E	15
126	43.12	13.83	129	28°	D	6, 7
127	43.12	13.62			E	6, 7
128	43.09	14.02	0	15°	B	6, 7, 10
129	43.05	13.89	40	20°	B	10
130	43.04	14.00			E	15
131	43.04	14.21	82	28°	D	6, 7
132	43.03	13.76	151	8°	D	15
133	43.01	14.16	106	25°	E	15
134	43.01	13.99	102	29°	D	6, 7
135	43.00	13.90			E	6, 7
136	42.98	14.11			E	6, 7
137	42.97	14.09			E	15
138	42.96	14.24	145	29°	D	6, 7
139	42.95	14.88			E	6, 7
140	42.94	14.23			E	6, 7
141	42.93	14.87			E	6, 7
142	42.93	13.86	104	12°	B	10
143	42.92	13.87			E	15
144	42.90	13.88	11	3°	C	10
145	42.9	14.24	89	22°	D	6, 7
146	42.89	14.53	173	29°	D	6, 7

Table 1. (continued)

Event	Latitude, °N	Longitude, °E	S_{hmin}	SD	Q	Source
147	42.86	14.42	23	19°	C	10
148	42.86	11.56	47	8°	A	4
149	42.85	11.71	115	31°	D	15
150	42.85	13.91	24	27°	D	6, 7
151	42.84	11.69	16	10°	C	4
152	42.84	14.16	14	10°	B	10
153	42.84	14.16			E	6, 7
154	42.84	14.16	147	6°	B	10
155	42.84	13.93	26	20°	C	6, 7, 10
156	42.83	11.57	99	24°	C	4
157	42.81	11.65	51	15°	C	4
158	42.81	14.38	135	21°	D	15
159	42.79	13.97	15	26°	D	6, 7
160	42.78	13.80	30	20°	C	6, 7, 10
161	42.78	13.98			E	15
162	42.77	14.43			E	15
163	42.73	11.92	13	31°	D	4
164	42.71	15.12			E	6, 7
165	42.69	14.00	124	14°	D	15
166	42.67	13.93	37	19°	D	6, 7
167	42.66	14.58	34	7°	A	6, 7, 10
168	42.66	14.15	1	5°	C	6, 7, 10
169	42.65	14.17	178	30°	D	6, 7
170	42.65	13.70	52	29°	D	6, 7
171	42.65	11.88	58	18°	C	4
172	42.62	14.07	49	26°	D	15
173	42.61	14.17	81	25°	D	15
174	42.61	13.98			E	6, 7
175	42.57	11.78	88	21°	C	4
176	42.56	11.87			E	4
177	42.55	13.80	45	31°	D	6, 7
178	42.55	11.84	66	5°	B	4
179	42.55	11.90	60	10°	B	4
180	42.55	13.87	179	11°	D	15
181	42.54	13.34			E	15
182	42.54	14.44	6	9°	D	6, 7
183	42.53	13.87	54	4°	B	6, 7, 10
184	42.5	13.88	48	23°	C	6, 7, 10
185	42.42	13.92	51	18°	B	6, 7, 10
186	42.42	14.09	75	14°	B	6, 7, 10
187	42.42	14.45	26	24°	C	10
188	42.42	13.86	53	12°	B	6, 7, 10
189	42.38	14.57	7	13°	D	15
190	42.35	12.21			E	4
191	42.35	14.77			E	6, 7
192	42.35	14.90	48	4°	B	6, 7, 10
193	42.25	14.31			E	6, 7
194	42.24	14.44			E	6, 7
195	42.24	14.28	70	16°	B	6, 7, 10
196	42.22	12.23	177	24°	D	4
197	42.21	12.14			E	4
198	42.21	14.51			E	6, 7
199	42.15	14.56	39	11°	B	6, 7, 10
200	42.13	14.70	37	16°	C	6, 7, 10
201	42.12	12.14	32	2°	D	4
202	42.12	14.65	70	22°	C	6, 7, 10
203	42.09	14.56	140	19°	C	6, 7, 10
204	42.07	14.39	65	4°	D	6, 7
205	42.06	14.29			E	6, 7
206	42.05	12.21	130	8°	D	4
207	42.03	15.20	58	27°	D	6, 7
208	41.97	14.94	19	10°	C	10
209	41.94	14.89	165	10°	D	6, 7
210	41.93	14.82	34	7°	B	10
211	41.91	14.75			E	15
212	41.89	14.80	8	20°	C	6, 7, 10
213	41.88	14.33			E	6, 7
214	41.88	14.30			E	6, 7
215	41.87	14.58	21	18°	D	6, 7
216	41.87	16.77			E	3, 5
217	41.77	15.07			E	15
218	41.70	14.15			E	6, 7
219	41.63	17.71			E	3, 5

Table 1. (continued)

Event	Latitude, °N	Longitude, °E	S_{hmin}	SD	Q	Source
220	41.61	14.84			E	6, 7
221	41.49	14.69	38	11°	A	3, 5, 10
222	41.47	14.76	47	18°	C	3, 5, 10
223	41.46	15.23	8	10°	C	3, 5, 10
224	41.45	16.93			E	3, 5
225	41.44	15.26			E	3, 5
226	41.41	16.72			E	3,5
227	41.38	14.85			E	3, 5
228	41.38	15.45			E	3, 5
229	41.38	15.35	36	27°	C	3, 5, 10
230	41.34	14.81	35	14°	B	3, 5, 10
231	41.34	15.49			E	3,5
232	41.32	15.35	72	18°	B	3, 5, 10
233	41.32	14.86	105	15°	D	3, 5
234	41.32	15.53			E	3, 5
235	41.32	14.62	69	8°	A	3, 5, 10
236	41.29	15.34	38	24°	C	3, 5, 10
237	41.28	15.21	112	26°	D	3, 5
238	41.26	15.48	76	4°	C	3, 5, 10
239	41.25	15.50	109	19°	D	3, 5
240	41.24	15.41			E	3, 5
241	41.23	15.58			E	3, 5
242	41.21	14.84	45	17°	B	3, 5, 10
243	41.19	14.93	169	8°	D	3, 5
244	41.16	15.59	13	15°	C	3, 5, 10
245	41.14	15.59	54	28°	C	3, 5, 10
246	41.14	13.69	56	11°	C	3, 5, 10
247	41.11	17.88			E	3, 5
248	41.10	15.67	13	23°	D	3, 5
249	41.09	15.67			E	3, 5
250	41.07	15.70	23	10°	B	3, 5, 10
251	41.06	16.21	64	25°	C	3, 5, 10
252	41.04	14.01	123	28°	D	3, 5
253	41.01	17.52			E	3, 5
254	40.96	15.85	68	12°	B	3, 5, 10
255	40.93	18.35			E	3, 5
256	40.93	15.14	30	19°	C	3, 5, 10
257	40.86	14.05			E	3, 5
258	40.79	14.44	76	25°	C	3, 5, 10
259	40.74	16.17	26	14°	B	3, 5, 10
260	40.63	15.70	59	11°	B	12
261	40.62	16.19			E	3, 5
262	40.61	16.29			E	3, 5
263	40.55	16.26			E	3, 5
264	40.55	16.34			E	3, 5
265	40.53	16.35			E	3, 5
266	40.52	16.36	35	31°	D	3, 5
267	40.50	16.35	158	21°	D	3, 5
268	40.48	16.56	56	25°	D	3, 5
269	40.48	16.31	26	13°	B	3, 5, 10
270	40.47	16.38	1	13°	C	3, 5, 10
271	40.46	15.80	41	12°	B	3, 5, 10
272	40.46	16.50			E	3, 5
273	40.44	16.52	1	17°	D	3, 5
274	40.43	16.46	68	10°	C	3, 5, 10
275	40.43	14.79	40	29°	D	3, 5
276	40.41	15.91	13	33°	D	3, 5
277	40.37	14.84	169	17°	B	3, 5, 10
278	40.35	15.85	53	11°	B	13
279	40.34	15.99			E	3, 5
280	40.34	15.93	52	11°	B	3, 5, 10
281	40.33	15.98	23	20°	D	3, 5
282	40.33	15.94	43	22°	C	3, 5, 10
283	40.32	16.03	42	24°	C	3, 5, 10
284	40.18	15.91			E	3, 5
285	39.73	16.59			E	6
286	39.71	16.62	4	16°	D	6
287	39.35	17.14	143	12°	C	6
288	39.26	17.16	58	25°	C	6
289	39.23	17.00	68	30°	C	6
290	39.14	17.30			E	6
291	38.97	17.16			E	6
292	38.96	17.21	127	12°	B	6

Table 1. (continued)

Event	Latitude, °N	Longitude, °E	$S_{h\min}$	SD	Q	Source
293	38.95	17.16	50	17°	C	6
294	38.88	17.15	46	30°	D	6
295	38.44	16.90	31	21°	C	6
296	37.89	12.53	30	20°	C	9, 10
297	37.85	12.56	58	22°	C	9, 10
298	37.68	12.58	91	28°	D	9
299	37.60	12.98	30	35°	D	9
300	37.48	14.54	126	12°	B	9, 10
301	37.45	14.74	156	13°	B	9
302	37.43	14.91	132	11°	B	9, 10
303	37.43	15.04	152	25°	C	9, 10
304	37.42	14.96			E	9
305	37.31	14.72	57	47°	E	9, 10
306	37.18	14.342	23	42°	E	9
307	37.14	14.32			E	2
308	37.12	14.30	110	13°	A	9
309	37.12	14.16	106	15°	B	9
310	37.11	14.48	17	57°	E	9
311	37.07	14.47			E	2
312	37.06	14.56	51	31°	D	9
313	37.04	14.35			E	2
314	37.01	14.07			E	2
315	37.01	14.05	94	13°	B	2, 10
316	37.01	14.72	46		E	2
317	37.00	13.85	131	7°	B	2, 10
318	36.98	15.23	76	14°	B	9, 10
319	36.94	15.12	41	12°	A	9, 10
320	36.95	14.54	138	38°	D	9
321	36.94	14.73			E	2
322	36.87	14.59	68	17°	B	9, 10
323	36.81	15.12	64	11°	B	9
324	36.78	15.07	62	15°	B	9, 10
325	36.77	15.01	54	52°	E	9, 10
326	36.70	13.46	0	30°	D	2
327	36.54	14.63			E	2
328	36.31	15.13	23	13°	B	2, 10
329	36.12	14.91	32	21°	B	2

[a] $S_{h\min}$, minimum horizontal stress; SD, standard deviation; Q, quality ranking [*Zoback*, 1992]. Sources: 1, *Montone et al.* [1992]; 2, *Cesaro* [1993]; 3, *Amato et al.* [1995]; 4, *Montone et al.* [1995]; 5, *Amato and Montone* [1997]; 6, *Montone et al.* [1997]; 7, *Mariucci et al.* [1999a]; 8, *Montone and Mariucci* [1999]; 9, *Ragg et al.* [1999]; 10, *Montone et al.* [1999]; 11, *Mariucci et al.* [1999b]; 12, *Mariucci et al.* [2002]; 13, *Cucci et al.* [2004]; 14, GNDT Project, 2000; 15, this work.

investigations, excluding the faults for which focal mechanisms are available.

2.1. Borehole Breakouts

[9] Borehole breakout data (Table 1) were incremented by about 50%, from 109 [*Montone et al.*, 1999] to 149 reliable stress indicators, thanks to cooperation between INGV and oil, gas and geothermal companies, as ENI-AGIP, ENEL (the National Electricity Authority), and also Enterprise Oil. In particular, ENI-AGIP in the two last years provided 68 new borehole records, relative to deep wells located in northern Italy (Lombardy, Emilia-Romagna, Veneto and Tuscany).

[10] Presently, our data set contains 329 deep wells (Table 1), with both paper and digital logs, 149 of which gave reliable results in terms of $S_{h\min}$ directions. The depth of the wells is down to 7.5 km and the average depth of breakout zones is 3–4 km. We adopted the quality ranking system proposed by *Zoback* [1992] mainly depending on total breakout length and standard deviation of the mean breakout direction [see also *Montone et al.*, 1999, Table 6]. This quality estimate is based on the statistical azimuthal distribution of the breakout data in the well. Then, we attribute quality A only to those wells with a breakout zone length greater than 300m and with a standard deviation of $S_{h\min}$ direction less than 12°. Quality A (the best) was assigned to 10 wells, 65 are of B quality and 74 have C quality.

[11] Data are spread over the entire Italian territory (except Sardinia where no wells were drilled) although they are not homogeneously distributed (Figure 1). Most of the new borehole data are located in the Po Plain (Lombardy region), where no (or only a few) other data are available to determine the stress field. We have a good concentration of data along the southern Apenninic belt, in the Campania and Basilicata regions, and along the Apenninic foredeep. Other large parts of Italy, as for example the Alps, the Calabria region and the central part of the Apenninic belt, are on the contrary rather poor in breakout data.

2.2. Focal Mechanisms

[12] Typical data used to compile a stress distribution map are earthquake fault plane solutions because they represent the seismic deformation and give information about the state of stress around a fault. To be sure to work with data that are the response to the regional stress field rather than deformation due to local effects, we use only well constrained focal mechanisms, obtained for events with

Table 2. Earthquake Focal Mechanism Data Set[a]

Event	Latitude, °N	Longitude, °E	S_{Hmin}	Q	TR	D	M	Date	Strike 1	Dip 1	Slip 1	Strike 2	Dip 2	Slip 2	Source
1	46.36	13.27	75	B	TF	10	6.4	5/6/1976	*282*	*23*	*119*	71	70	78	1
2	46.25	13.30	117	B	TF	10	4.9	5/7/1976	95	37	63	307	58	108	1
3	46.26	13.36	110	B	TF	10	5.1	5/9/1976	89	48	60	310	50	119	1
4	46.31	13.00	75	B	TF	10	5.0	5/11/1976	283	35	123	65	61	69	1
5	46.33	13.20	71	B	TF	10	5.3	9/11/1976	271	38	116	60	56	71	1
6	46.34	13.20	79	B	TF	10	5.6	9/11/1976	260	24	91	79	66	90	1
7	46.32	13.20	250	B	TF	10	5.9	9/15/1976	246	36	84	73	54	94	1
8	46.32	13.17	69	B	TF	10	6.0	9/15/1976	272	29	115	64	64	77	1
9	46.33	13.00	86	B	TF	12	5.2	9/16/1977	291	35	119	77	60	72	1
10	38.10	16.03	167	B	NF	33	5.2	3/11/1978	270	41	−72	66	52	−105	2
11	38.39	15.07	93	B	SS	14	6.0	4/15/1978	135	60	−176	43	86	−30	2
12	42.65	12.46	87	C	NF	10	4.4	7/30/1978	206	35	−49	340	65	−114	3
13	38.67	12.86	105	B	TF	9	4.9	1/20/1979	72	29	53	293	67	109	4
14	46.36	13.28	279	B	SS	10	4.7	4/18/1979	323	66	169	58	80	24	1
15	43.13	12.86	215	C	NF	10	4.1	5/21/1979	299	30	−98	128	61	−85	3
16	42.81	13.06	79	B	NF	16	5.8	9/19/1979	*183*	*28*	*−70*	341	64	−100	2
17	38.28	11.74	252	B	TF	33	5.3	12/8/1979	235	45	67	87	50	111	2
18	40.46	15.85	45	B	NF	24	4.8	5/14/1980	119	38	−112	326	56	−74	5
19	38.48	14.25	257	B	TF	14	5.7	5/28/1980	83	43	99	252	48	82	2
20	40.91	15.37	39	B	NF	10	6.9	11/23/1980	135	41	−80	*303*	*50*	*−98*	2
21	40.89	15.26	55	B	NF	10	5.0	11/24/1980	131	29	−110	333	63	−79	5
22	40.70	15.47	54	B	NF	10	4.9	11/25/1980	129	26	−65	281	67	−102	5
23	40.65	15.40	20	B	NF	10	5.4	11/25/1980	122	30	−119	335	64	−74	2
24	40.95	15.37	27	B	NF	15	5.2	1/16/1981	115	30	−93	298	60	−89	2
25	40.74	15.64	47	B	NF	33	4.5	11/29/1981	104	41	−138	340	64	−58	5
26	40.81	15.36	38	B	NF	10	4.7	8/15/1982	158	48	−45	282	59	−128	5
27	43.12	12.59	74	B	NF	13	4.6	10/17/1982	132	38	−137	6	65	−60	3
28	43.16	12.59	76	B	NF	16	4.6	10/17/1982	139	34	−129	3	65	−67	3
29	43.13	12.63	83	B	NF	19	4.6	10/18/1982	142	27	−131	7	70	−72	3
30	44.69	10.32	54	B	TS	37	5.0	11/9/1983	14	43	29	*262*	*71*	*129*	2
31	43.27	12.57	39	B	NF	14	5.6	4/29/1984	*143*	*21*	*−72*	304	70	−97	2
32	41.77	13.89	57	B	NF	10	5.9	5/7/1984	*174*	*31*	*−52*	312	66	−110	2
33	41.83	13.95	56	B	NF	13	5.5	5/11/1984	*156*	*43*	*−76*	317	49	−103	2
34	40.95	15.47	63	B	NF	10	4.5	1/28/1987	160	45	−79	326	46	−100	5
35	43.25	13.94	122	B	TF	12	5.1	7/3/1987	311	45	103	113	46	77	6
36	43.78	12.23	190	C	NF	11	4.5	7/5/1987	300	34	−63	88	60	−107	3
37	40.08	16.01	55	B	NF	10	4.7	1/8/1988	148	30	−86	324	60	−92	5
38	42.37	16.57	85	B	TF	24	5.4	4/26/1988	289	44	121	68	53	63	2
39	43.06	12.76	71	B	NF	33	4.6	12/22/1989	192	51	−43	312	58	−132	3
40	40.75	15.85	228	B	SS	26	5.8	5/5/1990	184	73	13	*90*	*78*	*162*	2
41	40.75	15.81	238	B	SS	15	4.8	5/5/1990	*282*	*83*	*173*	13	83	7	5
42	37.32	15.25	227	B	SS	10	5.6	12/13/1990	274	64	174	7	85	26	2
43	40.73	15.77	48	B	SS	8	5.1	5/26/1991	183	71	−9	*276*	*81*	*−160*	5
44	43.12	12.68	61	B	NF	10	4.6	6/5/1993	135	33	−112	342	59	−76	3
45	41.90	15.97	225	B	TF	10	5.2	9/30/1995	197	32	58	53	64	108	2
46	40.76	15.49	47	B	NF	10	4.9	4/3/1996	123	30	−110	325	62	−79	3
47	44.79	10.78	246	B	TF	10	5.4	10/15/1996	217	53	47	94	54	132	2
48	42.60	13.28	56	C	NF	10	4.3	10/20/1996	130	37	−113	338	57	−74	3
49	41.40	14.63	205	B	NF	10	4.5	3/19/1997	280	27	−110	122	65	−80	7
50	36.93	16.03	60	C	SS	33	4.5	3/25/1997	104	78	179	194	89	12	7
51	43.01	12.90	46	B	NF	10.2	4.5	9/3/1997	137	30	−88	315	60	−91	8
52	43.02	12.89	237	B	NF	10	5.7	9/26/1997	321	44	−98	*152*	*46*	*−83*	8
53	43.03	12.85	48	B	NF	10	6.0	9/26/1997	*144*	*42*	*−80*	312	49	−98	8
54	43.06	12.85	71	C	NF	10	4.3	9/26/1997	193	45	−43	316	61	−126	7
55	43.01	12.97	56	B	NF	10	4.5	9/26/1997	147	29	−88	325	61	−91	8
56	43.09	12.81	238	C	NF	5.5	4.3	9/27/1997	326	35	−92	148	55	−89	8
57	43.02	12.83	230	C	NF	10	4.2	9/27/1997	288	36	−135	160	66	−63	7
58	43.06	12.77	39	C	NF	10	4.3	9/27/1997	136	35	−80	304	56	−97	7
59	43.64	12.14	45	C	NF	10	4.4	10/2/1997	158	41	−58	298	56	−115	7
60	43.03	12.84	40	B	NF	10	5.2	10/3/1997	141	43	−74	300	49	−104	8
61	42.94	12.93	221	B	NF	10	4.7	10/4/1997	318	42	−80	125	49	−99	8
62	42.90	12.90	217	C	NF	10	4.4	10/4/1997	299	42	−101	133	49	−81	7
63	42.93	12.86	205	C	NF	10	4.4	10/4/1997	322	33	−52	99	64	−112	7
64	42.93	12.90	229	C	NF	10	4.4	10/4/1997	329	43	−77	131	48	−102	7
65	43.02	12.84	48	B	NF	10	5.4	10/6/1997	145	40	−80	312	51	−98	8
66	42.99	12.82	45	C	NF	11.6	4.2	10/7/1997	126	26	−102	319	65	−84	8
67	43.03	12.85	42	B	NF	10	4.5	10/7/1997	141	42	−77	304	49	−101	8
68	42.91	12.94	238	B	NF	10	5.2	10/12/1997	321	40	−100	154	51	−82	8
69	42.86	12.97	217	C	NF	10	4.3	10/12/1997	271	14	−133	136	80	−80	7
70	42.90	13.00	214	C	NF	10	4.3	10/13/1997	315	37	−73	115	54	−102	7
71	42.89	12.92	220	C	NF	10	4.4	10/13/1997	305	35	−96	133	56	−86	7
72	42.93	12.92	39	B	NF	10	5.6	10/14/1997	*122*	*38*	*−100*	314	52	−82	8
73	42.93	12.89	221	C	NF	10	4.4	10/15/1997	329	40	−65	117	55	−110	7

Table 2. (continued)

Event	Latitude, °N	Longitude, °E	S_{Hmin}	Q	TR	D	M	Date	Strike 1	Dip 1	Slip 1	Strike 2	Dip 2	Slip 2	Source
74	42.91	12.92	212	C	NF	10	4.3	10/16/1997	310	11	−80	120	79	−92	7
75	42.98	12.89	26	C	NF	10	4.1	10/16/1997	118	35	−88	295	55	−92	7
76	43.04	12.89	60	C	SS	10	4.4	10/16/1997	305	33	−123	163	63	−70	7
77	43.04	12.89	242	C	SS	10	4.3	10/16/1997	287	80	175	18	85	10	8
78	42.89	12.91	211	C	NF	10	4.2	10/17/1997	326	48	−53	97	54	−124	7
79	42.97	12.79	47	C	NF	10	4.2	10/19/1997	128	44	−103	326	47	−78	8
80	42.84	13.01	217	C	NF	10	4.3	10/25/1997	333	33	−54	112	64	−111	7
81	42.87	13.00	44	B	NF	10	4.9	11/9/1997	118	46	−113	329	48	−68	7
82	42.88	12.95	55	C	NF	10	4.3	11/30/1997	125	36	−119	339	59	−70	7
83	44.09	10.55	33	C	NF	10	4.3	12/24/1997	95	49	−132	329	56	−53	7
84	42.87	12.99	235	C	NF	10	4.3	12/31/1997	293	35	−135	164	66	−64	7
85	38.40	12.90	75	B	TF	10	4.8	1/17/1998	58	29	71	260	62	100	7
86	43.00	12.90	224	C	NF	10	4.4	2/7/1998	308	36	−98	138	55	−84	7
87	42.90	12.90	53	B	NF	10	5.0	3/21/1998	137	15	−97	325	75	−88	7
88	43.16	12.70	64	B	NF	10	5.1	4/3/1998	152	23	−80	321	68	−94	2
89	43.23	12.67	74	C	NF	10	4.3	4/3/1998	152	33	−108	352	59	−79	7
90	43.18	12.76	54	B	NF	10	4.8	4/5/1998	138	31	−98	327	59	−85	7
91	46.24	13.71	288	C	TF	10	4.3	5/6/1998	247	44	40	127	64	127	7
92	43.17	12.73	244	C	NF	10	4.3	6/2/1998	311	42	−124	173	56	−63	7
93	38.46	13.08	82	B	TF	10	5.2	6/20/1998	69	22	76	264	68	96	7
94	38.50	13.10	80	B	TF	10	4.6	6/21/1998	69	36	77	265	55	99	7
95	38.43	12.67	258	B	TF	10	4.6	6/21/1998	88	38	102	252	53	80	7
96	43.00	12.80	28	C	NF	10	4.0	6/25/1998	96	47	−123	319	52	−60	7
97	42.41	12.98	179	C	NF	10	4.4	8/15/1998	298	26	−52	76	70	−107	7
98	40.03	15.98	44	B	NF	10	5.6	9/9/1998	139	29	−83	311	61	−94	2
99	38.46	13.60	80	B	TF	10	5.0	9/14/1998	72	30	80	263	60	96	7
100	44.02	11.92	134	C	SS	33	4.4	1/25/1999	91	66	17	354	75	155	7
101	38.17	15.06	280	B	NF	33	4.7	2/14/1999	18	39	−108	220	53	−76	7
102	44.29	10.90	192	B	NF	10	4.7	7/7/1999	314	40	−44	80	64	−121	7
103	42.67	13.19	229	C	NF	10	4.2	10/10/1999	348	50	−47	112	55	−129	7
104	46.60	10.31	237	B	NF	10	4.8	12/29/1999	320	43	−99	152	47	−82	7
105	38.29	11.85	57	B	TF	10	4.8	12/30/1999	50	33	82	240	57	95	7
106	46.60	10.32	252	C	NF	10	4.1	12/31/1999	13	34	−45	143	67	−116	7
107	42.89	11.74	190	B	NF	10	4.5	4/1/2000	309	38	−49	81	63	−117	7
108	46.60	10.33	251	C	NF	5	4.0	4/6/2000	359	47	−64	144	49	−115	7
109	40.98	10.10	185	B	TF	10	4.8	4/26/2000	179	39	83	8	51	96	7
110	44.24	12.02	311	C	TF	10	4.2	5/2/2000	304	41	81	136	50	98	7
111	44.14	11.97	309	C	TF	10	4.1	5/6/2000	287	33	64	137	61	106	7
112	44.30	11.90	331	B	TF	10	4.6	5/8/2000	326	33	85	152	57	93	7
113	44.20	12.00	123	C	TF	10	4.3	5/9/2000	308	31	96	121	59	87	7
114	44.30	11.90	124	B	TF	10	4.8	5/10/2000	309	43	97	120	47	84	7
115	44.34	11.91	103	C	TF	10	4.2	5/11/2000	303	46	117	86	50	64	7
116	44.35	11.95	285	C	TF	10	4.4	5/12/2000	282	43	85	108	47	94	7
117	44.76	10.73	260	C	SS	5	4.4	6/18/2000	308	68	−161	210	73	−23	7
118	40.95	10.03	191	C	TF	10	4.3	6/27/2000	184	27	82	13	64	94	7
119	43.98	12.34	257	C	TF	10	4.3	8/1/2000	212	28	42	84	72	112	7
120	44.87	8.48	43	B	NF	10	4.9	8/21/2000	146	39	−71	302	53	−105	7
121	44.27	10.80	238	C	NF	10	4.2	10/3/2000	317	24	−105	153	67	−83	7
122	42.65	12.66	173	C	NF	10	4.2	12/16/2000	273	35	−76	76	56	−100	7
123	43.56	7.50	260	C	TF	10	4.4	2/25/2001	229	37	60	85	59	111	9
124	41.95	15.24	240	C	SS	10	4.3	7/2/2001	246	19	−166	143	85	−72	9
125	46.70	11.30	253	B	SS	10	4.7	7/17/2001	210	72	7	117	83	162	9
126	39.10	16.61	241	C	NF	10	4.4	10/18/2001	332	44	−88	149	46	−92	9
127	41.30	10.20	200	C	TF	10	4.3	11/7/2001	334	29	77	169	62	97	9
128	43.60	12.10	255	B	NF	10	4.7	11/26/2001	358	21	−72	158	70	−97	9
129	38.12	15.60	281	B	NF	10	7.0	12/28/1908	*349*	*42*	*−122*	209	55	−64	10
130	41.99	13.65	225	C	NF	8	6.9	1/13/1915	*135*	*63*	*−90*	315	26	−89	10, 11
131	41.05	15.36	2	C	NF		6.7	7/23/1930	280	50	−80	84	41	−101	12, 13
132	44.07	11.65	62	C	NF	7	4.7	2/11/1939	310	49	−120	171	49	−60	10
133	44.23	10.20	120	C	NF	27	4.9	10/15/1939	175	26	−126	33	69	−74	10
134	38.44	12.12	117	C	NF	20	6.9	3/16/1941	217	39	−76	19	52	−101	10
135	45.33	9.33	188	C	SS	6	5.0	5/15/1951	235	73	−171	142	81	−17	10
136	45.33	9.33	170	C	SS	6	4.5	5/16/1951	123	64	−17	220	74	−152	10
137	42.35	13.44	265	C	NF	10	5.0	6/24/1958	22	37	−57	162	59	−112	10
138	41.13	14.95	73	C	NF	8	5.7	8/21/1962	*310*	*65*	*−130*	201	54	−31	14
139	41.08	15.00	63	B	NF	8	6.1	8/21/1962	*310*	*65*	*−110*	186	41	−40	14
140	37.84	14.60	144	C	SS	38	5.0	10/31/1967	9	62	−169	273	80	−28	10
141	42.00	16.50	187	C	NF	33	4.7	12/9/1967	277	74	−90	97	15	−89	10
142	44.63	12.01	139	C	TF	33	5.2	12/30/1967	322	56	84	152	34	98	10
143	37.75	12.98	306	C	TF	10	5.4	1/15/1968	156	64	134	270	50	35	15
144	43.25	10.77	166	C	SS	33	4.7	8/19/1970	35	57	−156	291	70	−35	10
145	42.31	11.76	218	C	NF	2	4.6	2/6/1971	279	44	−133	151	59	−56	10
146	43.23	12.49	232	C	NF	33	4.5	2/12/1971	290	48	−139	169	60	−50	10

Table 2. (continued)

Event	Latitude, °N	Longitude, °E	$S_{h\min}$	Q	TR	D	M	Date	Strike 1	Dip 1	Slip 1	Strike 2	Dip 2	Slip 2	Source
147	41.20	15.24	207	C	SS	33	4.8	5/6/1971	252	85	5	161	85	174	10
148	40.34	15.77	248	C	SS	4	4.7	11/29/1971	23	84	6	292	84	173	10
149	42.82	12.93	250	C	NF	5	4.8	12/2/1974	195	48	−44	317	58	−128	10
150	41.65	15.73	237	C	SS	18	4.9	6/19/1975	281	71	168	14	78	19	10
151	44.75	9.52	185	C	NS	20	4.8	11/16/1975	312	62	−32	58	62	−147	10
152	42.67	12.46	184	C	TF	10	4.9	7/30/1978	199	41	112	350	52	71	10
153	40.80	16.11	245	C	NF	28	4.2	9/24/1978	333	71	−94	165	19	−78	10
154	44.41	11.99	210	C	NF	18	4.6	12/5/1978	330	45	−47	97	58	−124	10
155	39.33	16.19	126	C	NF	10	4.3	2/20/1980	43	43	−81	210	47	−98	10
156	43.57	12.22	5	C	NF	12.4	4.0	1/17/1993	75	40	−120	292	56	−67	16
157	37.98	14.14	65	B	TF	5	4.8	6/26/1993	204	31	40	78	70	115	17
158	44.13	10.17	35	C	SS	2	4.8	10/10/1995	80	80	170	171	80	10	16
159	44.33	10.55	111	C	SS	8.9	4.0	12/31/1995	155	55	−170	59	81	−35	16
160	46.40	13.40	103	B	SS	10	4.6	2/14/2002	55	61	2	324	88	151	9
161	38.50	14.70	90	B	TF	10	4.5	4/5/2002	57	23	54	275	71	104	9
162	39.61	16.82	348	B	SS	17	4.8	4/17/2002	123	56	−14	221	78	−146	9
163	40.70	15.70	229	C	NF	10	4.4	4/18/2002	335	33	−67	129	60	−104	9
164	45.60	14.20	271	C	SS	10	4.2	6/2/2002	316	84	176	46	86	6	9
165	44.60	10.70	264	C	SS	10	4.3	6/18/2002	218	52	13	120	80	141	9
166	38.40	13.80	54	B	TF	10	5.9	9/6/2002	255	49	121	34	50	60	9
167	38.40	13.80	50	B	TF	10	4.8	9/6/2002	240	44	104	41	47	77	9
168	38.90	14.20	39	C	TF	10	4.4	9/10/2002	8	34	54	229	63	112	9
169	38.40	14.00	49	B	TF	10	4.8	9/20/2002	24	47	56	250	53	122	9
170	38.40	13.70	44	B	TF	10	5.1	9/27/2002	35	45	77	233	47	103	9
171	38.36	13.74	251	B	TF	10	4.6	9/28/2002	84	42	107	242	50	75	9
172	38.40	13.80	58	B	TF	10	4.9	10/2/2002	20	45	42	258	62	127	9
173	37.78	15.03	287	C	SS	10	4.5	10/27/2002	329	71	161	66	73	20	9
174	37.70	15.10	179	B	SS	10	4.6	10/29/2002	312	75	−14	46	76	−165	9
175	41.75	14.94	44	B	SS	10	5.7	10/31/2002	178	80	−10	*270*	*80*	*−169*	9
176	41.76	14.85	37	B	SS	10	5.7	11/1/2002	*263*	*62*	*−164*	165	76	−29	9
177	41.71	14.81	28	C	SS	10	4.5	11/1/2002	252	74	180	342	90	16	9
178	41.71	14.79	27	B	SS	10	4.5	11/12/2002	251	78	−180	161	90	−12	9
179	43.95	11.96	242	B	NF	10	4.8	1/26/2003	321	21	−104	156	70	−85	9
180	43.20	15.49	102	B	TF	10	4.9	3/27/2003	72	50	48	307	55	129	9
181	43.15	15.51	108	B	TF	10	5.4	3/29/2003	92	47	67	303	48	112	9
182	43.10	15.30	275	C	TF	10	4.2	3/30/2003	119	38	120	263	58	68	9
183	43.10	15.30	104	B	TF	10	4.6	3/30/2003	285	38	92	103	52	89	9
184	44.80	8.90	255	B	SS	10	4.9	4/11/2003	300	71	−172	207	83	−19	9
185	43.34	15.75	108	B	TF	10	4.5	4/29/2003	108	38	90	289	52	90	9
186	41.68	14.80	33	C	SS	10	4.4	6/1/2003	168	74	−9	260	82	−164	9

[a] $S_{h\min}$, minimum horizontal stress; Q, quality ranking [*Zoback*, 1992]; TR, tectonic regime; NF, normal fault; SS, strike-slip fault; TF, thrust fault; TS, thrust to strike fault; NS, normal to strike fault; D, depth (km); M, magnitude (see references for different magnitude scales). Strike, dip, and slip, the assumed fault plane in italics. References: 1, *Pondrelli et al.* [2001]; 2, *Dziewonski et al.* [2000] and references therein; 3, this study and GNDT Project (Probable earthquakes in Italy between year 2000 and 2030: Guidelines for determining priorities in seismic risk mitigation, 2000, available at http://gndt.ingv.it/Att_scient/Pe2000_RelAnn/Amato/RelAnn_PE2000_Amato_Parte2.pdf); 4, *Pondrelli et al.* [1999]; 5, *Cucci et al.* [2004]; 6, *Pondrelli et al.* [1998]; 7, *Pondrelli et al.* [2002]; 8, *Ekström et al.* [1998]; 9, QRCMT (http://mednet.ingv.it/events/QRCMT/Welcome.html); 10, *Gasparini et al.* [1985]; 11, *Ward and Valensise* [1989]; 12, *Selvaggi et al.* [1997]; 13, *Boschi et al.* [1997]; 14, *Westaway* [1987]; 15, *Anderson and Jackson* [1987] 16, *Frepoli and Amato* [1997]; 17, *Azzara et al.* [1993].

$M \geq 4.0$ for the last 25 years and at least $M \geq 4.5$ for older earthquakes. Moreover, in order to have a homogeneous data set, we generally prefer the CMT-like solutions with respect to other proposed focal solutions. The *Zoback* [1992] criteria are used for selection, taking into account only events within the crust, their magnitude, and how they have been determined. However, fault plane solutions are never A quality since, according to *McKenzie* [1969], P and T axes of an individual earthquake may differ significantly from the actual stress orientation producing the slip. We then attribute B quality only to fault plane solutions of events with $M \geq 4.5$, C quality to those with $4.0 \leq M < 4.5$. We do not take into account fault plane solutions with D and E quality; focal mechanisms for lower magnitudes are considered only when used to compute stress inversions (see section 2.3).

[13] The characterization of stress regime and the determination of the $S_{h\min}$ direction can be based on the P, T, and N axes directions [see *Montone et al.*, 1999, Table 5], consistent with the World Stress Map assumptions [*Zoback*, 1992] or alternatively, by looking at the slip vector azimuth [*McKenzie*, 1969; *Michael*, 1987]. This second method is particularly appropriate when the focal plane solution shows a remarkable component of oblique slip and when the fault plane is known. However, in our data set it is possible to solve the nodal plane ambiguity and identify the slip vector direction only for 19 earthquakes out of 186, and with a large uncertainty, due to the complexity of these sources (the assumed fault planes are in italics in Table 2). 13 slip vectors, according to the stress regime characterization [*Zoback*, 1992], are relative to dip-slip faults (NF or TF), 1 is relative to predominately thrust with strike-slip component fault (TS) and 5 are relative to strike-slip faults (SS). Moreover, 9 out of 13 dip-slip nodal planes show almost pure dip-slip mechanisms (Table 2), where T axis (or P axis, if thrust) direction and slip vector azimuth roughly coincide

Table 3. Formal Inversions of Stress Axes[a]

Site	Latitude, °N	Longitude, °E	S1 azim/dip	S2 azim/dip	S3 azim/dip	*N*	Mis.	R	Depth, km	Period	*M*	Q	TR	Source
AMP	46.55	12.67	339/19	119/65	244/15	20	4.9°	0.4	4–19 (10–13)	1984–1998	2.8–5.6	B	SS	1
TOL	46.47	13.17	166/10	65/47	265/42	25	6.8°	0.3	4–19 (10–13)	1984–1998	2.8–5.6	B	TS	1
BOV	46.38	13.7	353/05	237/79	084/10	24	7.1°	0.6	4–19 (10–13)	1984–1998	2.8–5.6	B	SS	1
CL	46.33	12.58	140/00	230/05	045/85	30	5.4°	0.4	4–19 (10–13)	1984–1998	2.8–5.6	B	TF	1
GE	46.3	13.3	004/04	94/03	225/85	30	5.4°	0.4	4–19 (10–13)	1984–1998	2.8–5.6	B	TF	1
MN	46.25	12.95	166/07	76/04	319/82	32	5.1°	0.5	4–19 (10–13)	1984–1998	2.8–5.6	B	TF	1
ALP	46.17	12.33	163/15	255/08	011/73	25	5.9°	0.4	4–19 (10–13)	1984–1998	2.8–5.6	B	TF	1
BA	46.05	13.6	011/02	263/83	101/06	27	6.7°	0.6	4–19 (10–13)	1984–1998	2.8–5.6	B	SS	1
CC	44.97	10	049/00	319/60	139/30	14	7°	0.3	0–25	1988–1995	2.5–4.8	B	SS	2
AE	44.7	7.7	282/05	180/22	023/67	14	4.7°	0.6	0–25	1977–1993	2.7–4.8	B	TF	3
AW	44.5	7	054/66	160/07	253/23	16	5.3°	0.5	0–25	1959–1993	2.5–5.3	B	NF	3
CF	44.12	12.12	045/00	135/82	315/09	59	10°	0.4	0–25	1988–1995	2.5–4.8	B	SS	2
UM	43.25	12.75	342/86	129/02	219/01	19		0.4	0–15	1987	0.8–2.1	C	NF	4
VU	42.8	11.8	143/30	293/57	045/14	67	5.9°	0.8	0–8	1984–1990	1.5–4.2	B	SN	5
AL	41.7	12.7	321/49	131/40	225/05	45	8.3°	0.7	0–7	1989–1990	1.5–4.2	B	NS	5
GA	41.7	15.67	130/73	310/17	040/00	17	5.9°	0.5	14–24	1988–1995	2.5–4.8	B	NF	2
AI	38.5	15	342/13	236/50	082/37	25	7.0°	0.7	0–25	1988–1995	2.5–4.8	B	SS	2
SCW	38.3	15.8	040/53	188/32	288/16	16	5.9°	0.5	0–25	1988–1995	2.5–4.8	B	NF	2
SCE	38.3	16.7	134/01	040/74	224/16	9	3.9°	0.3	0–25	1988–1995	2.5–4.8	B	SS	2
SIC	38	15.5	143/73	026/08	293/15	20	4.6°	0.6	0–50	1968–1991	>2.5	B	NF	6

[a]Site, locations in Figure 2; *N*, number of events used for computation; Mis., mean misfit angle; R, stress ratio (s2 − s3)/(s2 − s1); Q, quality ranking [*Zoback*, 1992]; TR, tectonic regime: NF, normal fault; TF, thrust fault; SS, strike-slip fault; NS, normal to strike fault; SN, strike to normal fault; TS, thrust to strike-slip fault; Sources: 1, *Bressan et al.* [2003]; 2, *Frepoli and Amato* [2000a, 2000b]; 3, *Eva et al.* [1997]; 4, *Boncio et al.* [1996]; 5, *Montone et al.* [1995]; 6, *Caccamo et al.* [1996].

(maximum difference 9°); the other 4 have an oblique component in the slip (differences from 15° to 30°).We have substituted in our data set the $S_{h\min}$ azimuth derived from *T* axis with the value of 14 slip vector directions in order to verify possible changes in the active stress field orientation in the smoothed maps (see section 4) (we do not consider slip vectors for SS faults). The results show that considering the large amount of events (186) and the characteristics of our data set (150 out of 186 show a prevalent dip-slip component), the use of principal axis directions (*P*, *T*, and *N* axes) can provide a reliable description of the regional stress orientation.

[14] With respect to the previous compilation [*Montone et al.*, 1999], we have now 108 more data, reaching a total number of 186 (Figure 2 and Table 2), exclusively due to the contribution from the European-Mediterranean RCMT Catalog solutions (http://www.ingv.it/seismoglo/RCMT). We selected 57 events, occurred between 1997 and 2000, from *Pondrelli et al.* [2002]; 27 events between 2001 and 2003, from Quick RCMT data set, rapid moment tensor solutions that after a revision enter definitively in the RCMT Catalog (http://mednet.ingv.it/events/QRCMT/Welcome.html); several new moment tensors collected from other works [*Pondrelli et al.*, 1999; *Cucci et al.*, 2004; GNDT Project, Probable earthquakes in Italy between year 2000 and 2030: Guidelines for determining priorities in seismic risk mitigation, 2000, available at http://gndt.ingv.it/Att_scient/Pe2000_RelAnn/Amato/RelAnn_PE2000_Amato_Parte2.pdf]. Thus, in our collection 155 data from focal mechanisms obtained from waveform inversion (CMTs, RCMTs and other moment tensors) of earthquakes with magnitude between 4.0 and 6.0, occurred between 1976 and 2003, are now included together with 31 focal mechanisms obtained from first arrival wave polarities for events with magnitude between 4.5 and 7.0, occurred between 1908 and 1995 (from events 129 to 159 in Table 2).

[15] This study adds many new earthquake data in the entire study region, but the increase is particularly pronounced in the northern and southern Apennines and along the southern Tyrrhenian Sea.

2.3. Stress Inversions

[16] Stress direction determined from inversions of *P*, *T*, and *N* axes of diffuse seismicity is considered the most consistent information from seismological data, but past Italian seismicity rarely had enough density to allow these studies. We updated stress directions determined from formal inversions of our previous compilation [*Montone et al.*, 1999] and included some more recent data shown in Figure 2 and in Table 3 (from 9 to 20 data).

[17] For northeastern Italy, several stress direction values have been determined on local seismicity that occurred between 1984 and 1998 with magnitude ranging from 2.8 to 5.6 [*Bressan et al.*, 2003]. These data increase the coverage for this region, where only moment tensors for the 1976–1979 Friuli seismic sequence were available [*Pondrelli et al.*, 2001]. For southern Italy we added new data for the Gargano Promontory, Calabria and Sicily regions determined from background seismicity recorded by the INGV National Seismic Network [*Frepoli and Amato*, 2000a, 2000b].

2.4. Faults

[18] Unfortunately, the fault data set is still poor even though, compared to the previous paper [*Montone et al.*, 1999], it increased from 4 to 7 data (Table 4 and Figure 3). Although new paleoseismologic studies have been performed, only a few published data are available from which we can extract further information (fault slip vectors). Two fault data are located in the central Apennines [*Pantosti et al.*, 1996; *D'Addezio et al.*, 2001], one is in the southern Apennines [*Benedetti et al.*, 1998] and the remaining fault

Table 4. Fault Data[a]

Event	Latitude, °N	Latitude, °E	$S_{h\min}$	Q	TR	Source
1	42.18	13.48	55	C	NF	*Pantosti et al.* [1996]
2	39.85	16.2	30	C	NF	*Michetti et al.* [1997]
3	39.82	16.25	65	C	NF	*Cinti et al.* [1997]
4	40.4	15.75	40	C	NF	*Benedetti et al.* [1998]
5	39.4	16.25	85	C	NF	*Cucci and Valensise* [1995]
6	41.87	14.01	50	C	NF	*D'Addezio et al.* [2001]
7	38.36	16.01	130	C	NF	*Galli and Bosi* [2002]

[a] $S_{h\min}$, minimum horizontal stress; Q, quality ranking [*Zoback*, 1992]; TR, tectonic regime: NF, normal fault.

data are in Calabria [*Cucci and Valensise*, 1995; *Cinti et al.*, 1997; *Michetti et al.*, 1997; *Galli and Bosi*, 2002]. The three new data refer to three fault structures evidenced either from geomorphologic studies (event 5 in Table 4) or from paleoseismologic trenches (events 6 and 7 in Table 4). Since all these faults are reported as normal faults by the authors, without any detailed indication on the slip direction, we assume the $S_{h\min}$ direction as perpendicular to the fault strike, assigning quality C [*Zoback*, 1992]. As mentioned above, we do not include in this group faults for which seismic or geodetic focal mechanisms are available.

3. Stress Map

[19] About four years after the previous publication [*Montone et al.*, 1999], this new map provides a clearer view of the state of active stress in Italy (Figure 3), confirming some of the main features that were already outlined, and pointing out some new findings in poorly sampled regions. Concerning seismicity data, updated until 2003 for $M \geq 4.0$, the improvement is evident in all the study region, but is particularly pronounced in the northern and southern Apennines, in the Adriatic Sea and along the southern Tyrrhenian Sea. In the northern Apennines, the greatest contribution comes from the analysis of the 2000 Forlì (Emilia-Romagna region) seismic sequence (events 110–116 in Table 2), that allow to map with continuity the compression along its outer front. A compressional stress regime in the Adriatic microplate is also evident from new earthquakes in the Central Adriatic Sea. The new data in the southern Apennines confirm the results of previous studies that the whole area is characterized by NE-SW oriented extension; most of the mechanisms are normal faulting even if in the foredeep region (eastern sector) there is an area which shows strike-slip focal mechanisms. Several well constrained data, including those belonging to the 2002 Molise seismic sequence (events 175–178 and 186 in Table 2) (S. Pondrelli et al., Fast determination of moment tensors for the recent Molise (southern Italy) seismic sequence, *ORFEUS Electronic Newsletter*, *5*(1), 2, 2003, available at http://orfeus.knmi.nl/newsletter/vol5no1/molise.html), can now better support the presence of this stress regime, while in the older compilation only one strike-slip focal mechanism was present. In the Tyrrhenian offshore, north of Sicily, an E-W belt with thrust events pointing out approximately N-S compression is well evident. This trend is also highlighted by the events of the seismic sequence that started with the 6 September 2002 M_L = 5.6 earthquake occurred about 40 km NE of Palermo (Table 2).

[20] Seismicity data are almost uniformly distributed along the Apennines belt axis, from the northern Apennines to the Calabria-Sicily region, showing mainly normal faulting focal mechanisms. This extensional seismic belt is characterized by homogeneous stress directions and regimes (consistently shown by both earthquake fault plane solutions and breakouts) located in a very narrow zone (about 50 km wide) and clearly distinct from the prevailing compressional external zone, now well depicted by new data. Data indicating compression are localized along the outer Apenninic arc (from the Po Plain to Ancona, about 43.5°N and 13.5°E), in the Friuli seismic area and north of Sicily. Part of the Italian seismicity is related to volcanic areas, evident along the Tyrrhenian coast from Tuscany to Rome. In these areas, $S_{h\min}$ directions show a variable trend, which reflect the heterogeneous conditions of the stress field under the volcanic complexes; however an approximately NE-SW prevailing $S_{h\min}$ direction can be noted.

[21] For the part of the Italian territory that is not affected by crustal seismicity (Figure 4), borehole breakouts, geologic and structural data [*Meletti et al.*, 2000] are the main sources of information. For instance, along the Apenninic foredeep, breakout data cover a region that is not sampled by other stress indicators. In the Po Plain, both along its southern border and in its inner part, where most of the new data are located, the distribution of $S_{h\min}$ directions seem to follow the geometry of buried arcs [*Montone and Mariucci*, 1999], showing a complex pattern. Moving southward, $S_{h\min}$ directions show a sudden rotation from NW-SE to NE-SW, also shown by earthquake focal mechanisms that we relate to a regional change of tectonic regime, probably due to a lithospheric process. The NE-SW $S_{h\min}$ directions are found also along the southern Apennine foredeep.

[22] In the inner Calabrian arc, $S_{h\min}$ directions mainly deduced by earthquakes and surface faulting data depict quite well the arc geometry, with extension perpendicular to the arc; moving from north to south, an extensional regime with directions from NE-SW, E-W to WNW-ESE, can be observed. The outer Calabrian arc is almost exclusively sampled by borehole breakouts, but these unfortunately show inhomogeneous $S_{h\min}$ directions, not univocally interpretable. The few earthquake fault plane solutions suggest the presence of a strike-slip regime characterized by an approximately NE-SW $S_{h\min}$ and NW-SE $S_{H\max}$ directions. In Sicily, breakouts along the foredeep and foreland show two prevailing $S_{h\min}$ directions, approximately NW-SE and approximately ENE-WSW, respectively.

4. Smoothed Stress Maps

[23] Several smoothed stress maps have been constructed using the best active stress indicators in order to show mean stress directions and dominant stress regime for clusters of

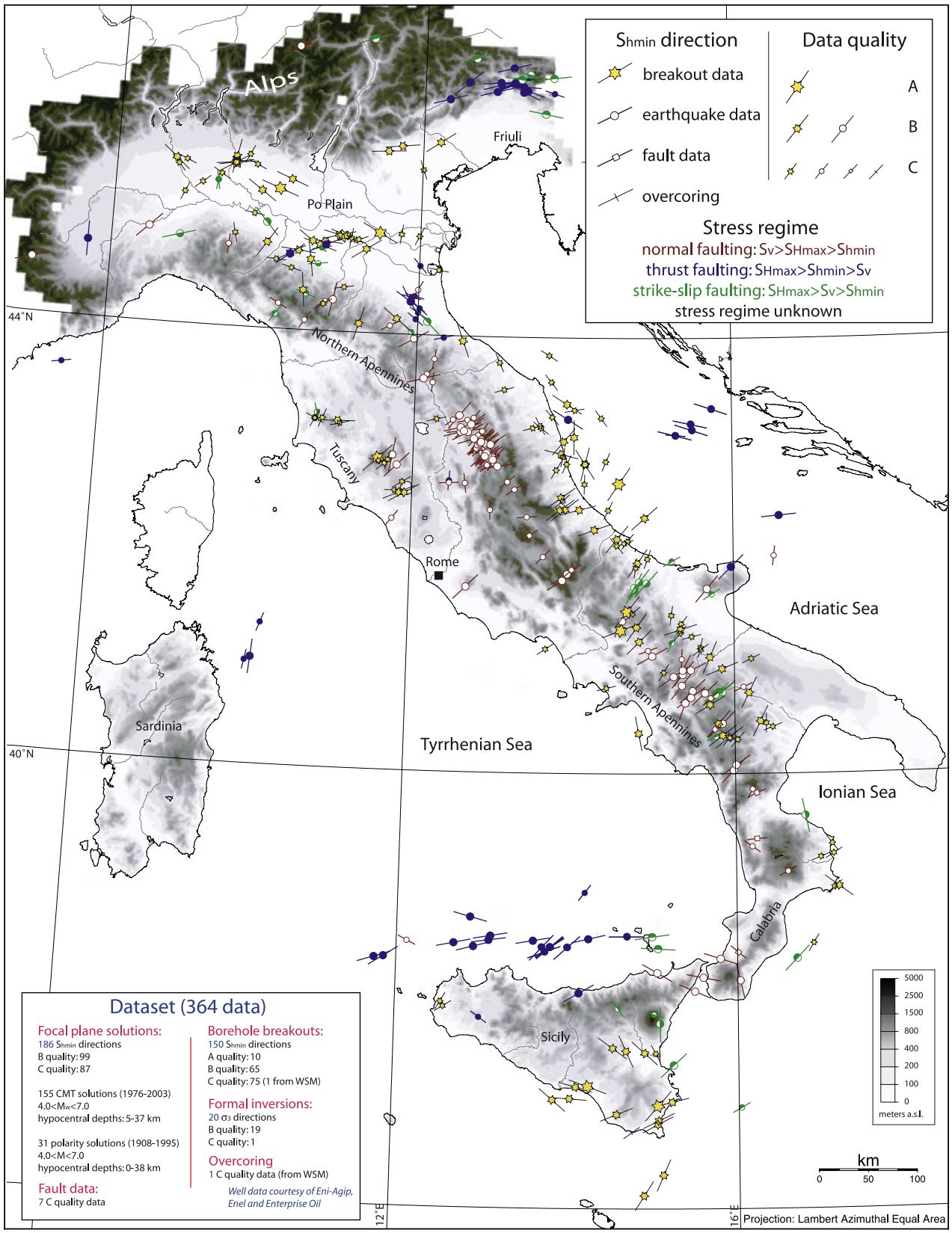

Figure 3. Active stress map of Italy with minimum horizontal stress orientations. See enhance version of this figure in the HTML

Table 5. Main Parameters for Smoothing Procedure

	L (Smoothing)	*A* (Search Radius), km
Suggested[a]		
Local maps	0.5–1	60–200
Regional maps	2–3	>400
In		
Figure 5a	1	90
Figure 5b	11	90
Figure 5c	1	30
Figure 5d	1	200

[a]After *Müller et al.* [2003].

data. Because of the dense spacing distribution of this data set with respect to the previous one [*Montone et al.*, 1999], the application of a smoothing algorithm provides a tool to highlight large-scale patterns and to eliminate local perturbations within the observed orientations. Moreover, it is useful to determine prevailing patterns of oriented data in places where they are sparse. That is done to compare the results with the complex tectonic setting of Italy and to examine the relationships between the state of stress of the Italian region and the central Mediterranean geodynamics.

[24] We analyzed horizontal stress directions in the Italian peninsula and surrounding regions applying the smoothing procedure due to *Müller et al.* [2003], using a software provided by Karlsruhe University researchers. The smoothing code, developed by *Wehrle* [1998], is based on the statistical smoothing algorithm of *Watson* [1985], the smoothing procedure for tectonic stress data of *Hansen and Mount* [1990], and the distance weight of *Hüsges* [1995]. The algorithm first places a regular grid over the study area and then calculates stress orientation for each grid point by considering data within a certain radius around the grid point itself. The main parameters that must be chosen are the smoothing parameter *L*, which balances the smoothness of the interpolation and the fit to the original data, and the search radius *A*, which defines the distance around the grid point where data are taken into account (Table 5). Other parameters can be used to select data points on the base of their amount and quality within the search area around a grid point; for example, if the data are less than a given threshold they are skipped. The data are weighted by their previously attributed quality and by the distance from the grid point, following a method which is independent on data distribution [*Müller et al.*, 2003].

[25] We have integrated our data set with part of the World Stress Map database taking into account 921 $S_{h\min}$ directions (only A, B and C quality): 362 from our data set and 559 from the World Stress Map database 2003 release (J. Reinecker et al., The 2003 release of the World Stress Map, 2003, available at http://www.world-stress-map.org) for regions around Italy (between 35°–49°N and 5°–21°E). We run the smoothing code over an area wider than the study region to improve the reliability of the smoothing inside the zone of interest and at its borders. We used a grid spacing of 0.25° for longitude and of 0.2° for latitude. The necessary parameters were chosen to smooth out local variations in the stress map while preserving significant short wavelength variations (Table 5). Figure 5a is the smoothed stress map that we consider the most representative of the main patterns of active stress in Italy; after several trials, we chose a search radius value *A* of 90 km, a degree of smoothing *L* equal to 1, and we use only grid values with at least one data point of A or B quality (or two quality C data) inside the area defined by the search radius. Comparing Figures 5a and 5b, we can evaluate the loss of information produced by a higher degree of smoothing in a region with a complex tectonic setting. Figures 5c and 5d show two examples to explain why a radius of 90 km better describes the Italian active stress conditions. A smaller radius provides maps well related to the data set but without further information on regional stress; a larger radius makes the stress directions more homogeneous but hides most of the short wavelength variations which are common in this region.

[26] In order to verify possible changes in the smoothed stress map, due to the use of different methods to evaluate $S_{h\min}$ orientation (see section 2) and different weights for some kind of data, we built up a new map applying the same smoothing parameters of Figure 5a to a modified data set. We have considered the slip vector azimuths, instead of *T* axis, for 14 focal mechanisms whose nodal plane ambiguity was solved, improving their quality rank (from B to A or from C to B). Moreover, we also increased fault quality (from C to A) to give more relevance to this kind of data. We did not observe any variation with respect to the previous map, probably due to the small differences between *T* axis and slip vector azimuth in most of data and to the low number of fault data.

5. Discussion

[27] The stress data are used, besides the computation of the smoothed directions, to assign a stress regime to the different regions, based mainly on fault plane solutions data, where available, and on the results of *Mariucci and Müller* [2003]. Our goal is to create a map showing the Italian regional stress field (orientation and regime) based on well constrained data for which the quality was already indicated in literature or definable by our analysis.

[28] The only previous interpolated map of the active stress field was proposed by *Rebaï et al.* [1992] showing the average stress orientations and regime for the entire Mediterranean region. In particular, concerning the Italian territory, available data were mainly due to earthquake focal mechanisms ($M > 3$), Quaternary microtectonic data and subordinately to in situ stress measurements. Most stress indicators were located along the southern Apennines and in Sicily, in the other regions almost no data were available. Therefore the interpolated map is affected by large uncertainties both in direction and in regime of the stress field. With our new data set (updated to 2003) we cover a large part of Italy better defining regime and orientations of different tectonic domains (Figure 6). Large differences in tectonic regime and orientation are well evident with respect to the previous interpolated maps [*Rebaï et al.*, 1992; *Bassi et al.*, 1997] in particular along the southern Apennines foredeep, northern Sicily offshore, in Calabria and also in the northern Apennines.

[29] In order to see how our interpretations match and to make inferences on the type of earthquakes that we can expect in the future in Italy, we overlap the smoothed stress map (Figure 6) to the database of *Valensise and Pantosti* [2001]. It contains a compilation of historical

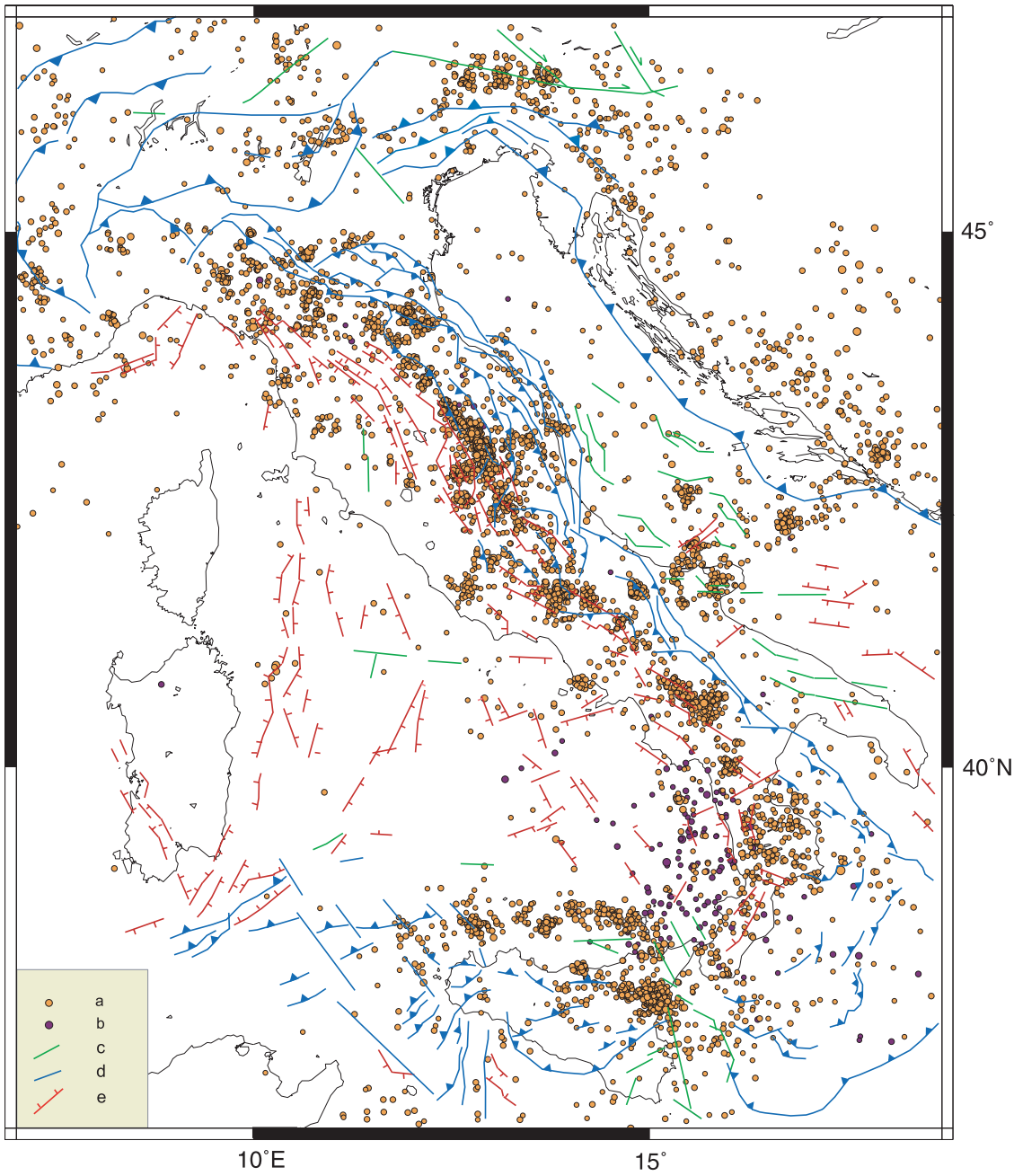

Figure 4. Seismicity and tectonic setting of the region. Legend a and b are crustal and deep earthquakes scaled by magnitude from INGV catalogue (period from 1983 to 2003, $M > 3$); c, d, and e are strike-slip, thrust, and normal faults simplified from *Meletti et al.* [2000].

seismogenic sources derived from intensity data and geological/geophysical sources, covering only the seismically active regions of Italy where moderate to large earthquakes have occurred (from approximately 1000 to 1997). Geological and geomorphologic data point out recent tectonic regime (i.e., Pleistocene and Holocene), but they do not always clarify the present one, which in some Italian regions has possibly changed very recently [*Patacca and Scandone*, 1989; *Westaway*, 1993]. In Figure 6 we have chosen to plot on the smoothed stress map only the "well constrained" seismogenic sources (according to *Valensise and Pantosti* [2001]). Our data set is almost completely independent from this one, except for a few seismic events, allowing a significant comparison. We make hypotheses on the kind of earthquakes that the determined stress field could activate, being the geometry of potential seismic sources relatively well known.

[30] Starting from northwestern Italy, we find a complex pattern of stress directions which at first approximation follows the arc shape of the Alps. Figure 6 suggests thrust or strike-slip earthquakes of moderate size along the outer front of the belt. In northeastern Italy, most of our knowledge on the kinematics and the stress in the region comes from focal mechanisms of the 1976 Friuli sequence and

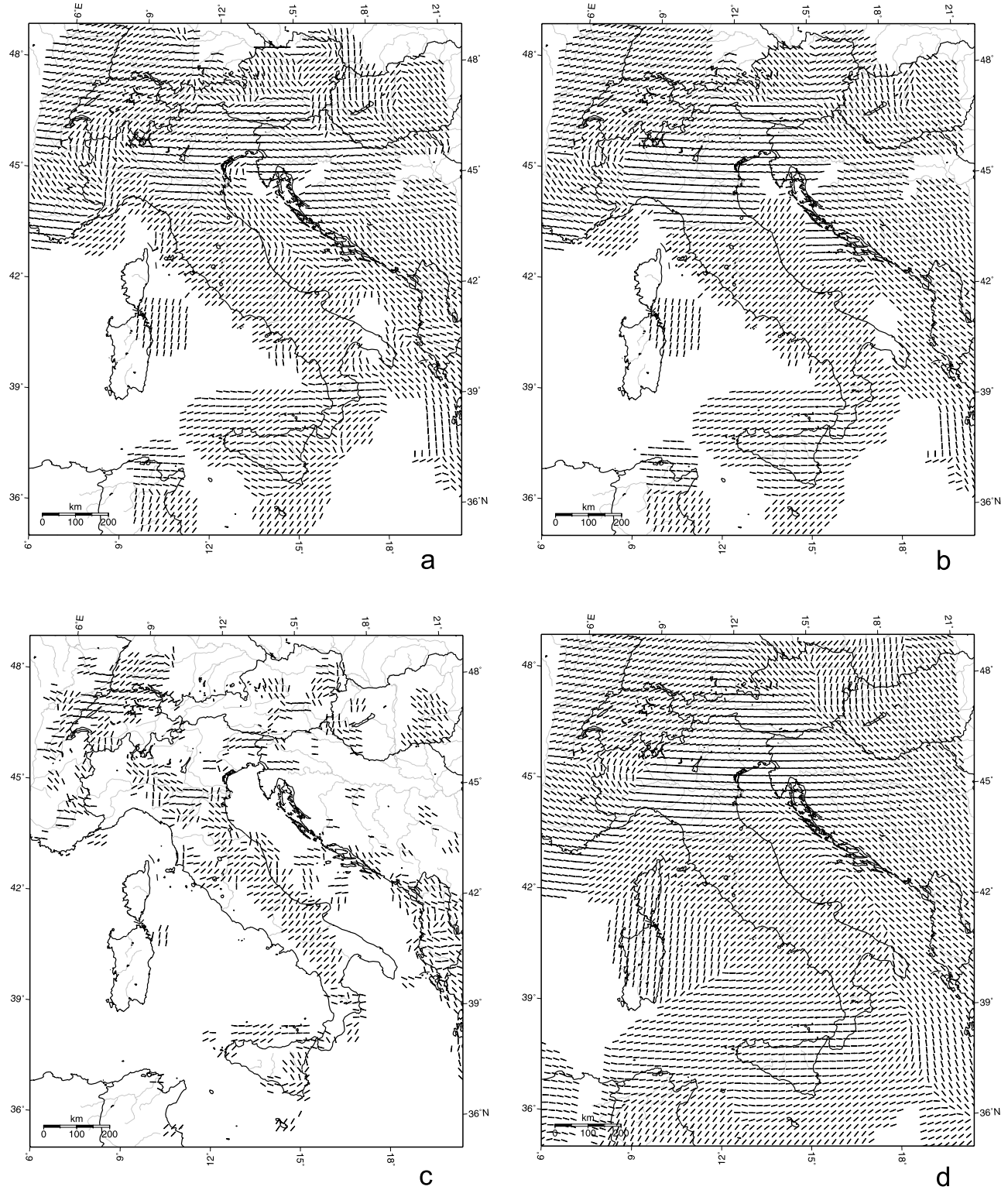

Figure 5. Four examples of smoothed stress maps for different choices of parameters. Short line segments are estimates of the minimum horizontal stress directions. (a) Smoothing parameter $L = 1$, search radius $A = 90$ km; (b) $L = 11$, $A = 90$ km; (c) $L = 1$, $A = 30$ km; (d) $L = 1$, $A = 200$ km. See text and Table 5 for details.

successive seismicity. Other faults are hypothesized for the south Alpine front on the basis of geology and geomorphology, and in some cases with historical (intensity) data. The trend of these faults is parallel to the foot of the mountain belt (WSW-ENE, E-W, and NW-SE going from west to east). The smoothed stress directions, constrained by fault plane solutions in Friuli and breakouts to the west, show a similar, although gentler, rotation, suggesting

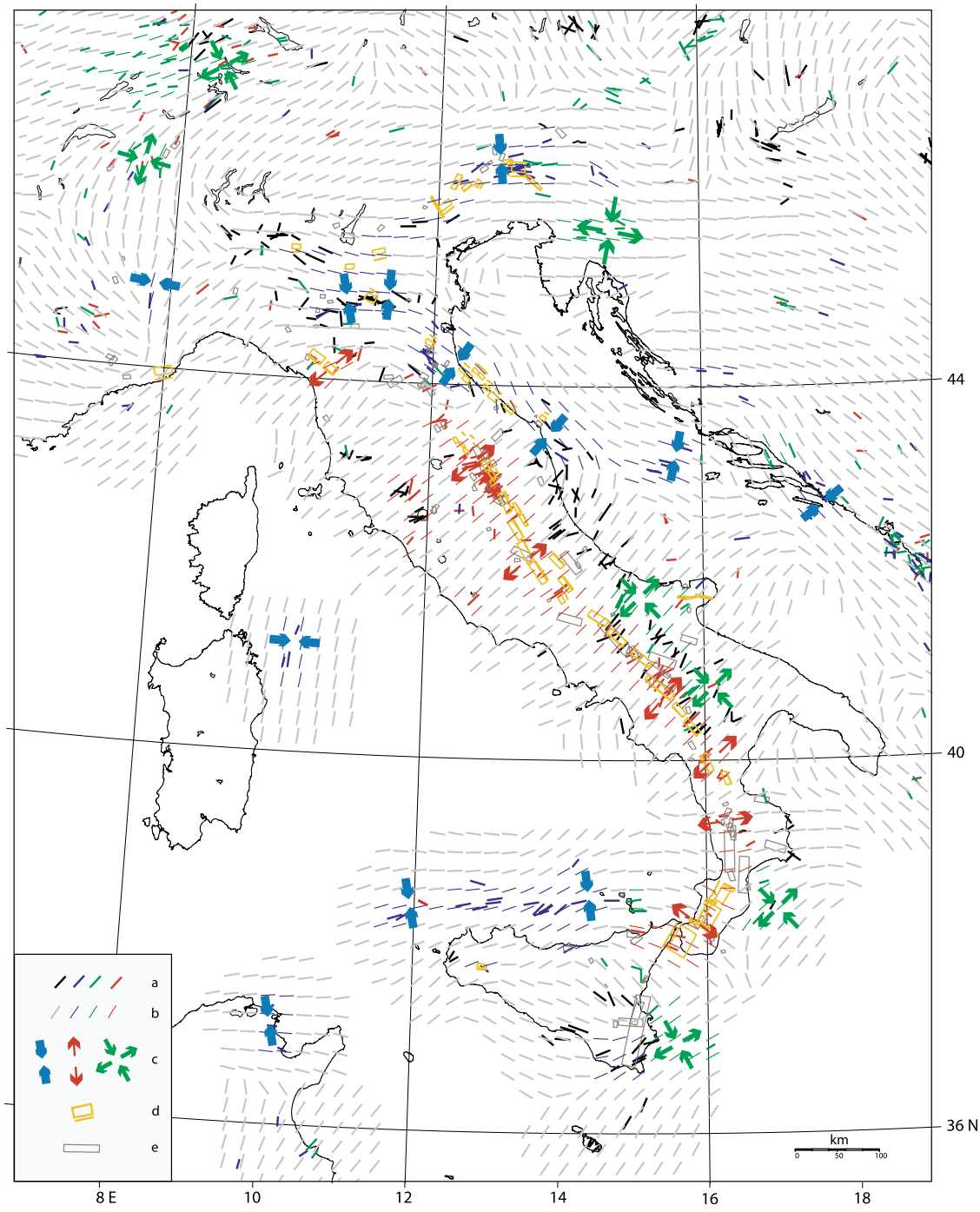

Figure 6. Smoothed $S_{h\min}$ orientation and stress regime of Italy. Legend a indicates $S_{h\min}$ directions from our data set and the World Stress Map 2003 release (colors mean different tectonic regimes: black is unknown, blue is compressional, green is strike-slip and red is extensional regime); b indicates smoothed stress directions from Figure 5a (colors as before); c indicates direction of inferred regional stress regime (colors as before); and d and e indicate integrated seismogenic sources [from *Valensise and Pantosti*, 2001] from geological/geophysical (yellow) and well constrained historical (grey) data.

activation of these faults as thrust or reverse (Figures 4 and 6). Strike-slip earthquakes along the transverse faults reported by *Valensise and Pantosti* [2001] are also possible.

[31] Very few earthquakes occurred in the Po Plain where major information on the stress directions derive from breakout data. In this area, many breakouts clearly evidence the presence of a general N-S compression modulated by short wavelength variations which follow the buried thrust fronts [*Montone and Mariucci*, 1999]. The variations observed in the deep wells are probably influenced by shallow effects, at least in the upper crustal layers, that include the weight of the overburden, the shallow thrust

structures beneath the plain and the presence of secondary structural arcs [*Doglioni*, 1991; *Mariucci et al.*, 1999b]. However, since the few earthquakes occurred in this region are generally located at depths of 10–20 km [*Selvaggi et al.*, 2001] and considering that the *T* axis orientations are in agreement with breakout data, we can speculate that breakout results reflect the regional pattern, i.e., the N-S compression. This stress orientation is also consistent with the activation of E-W trending thrust or reverse faults [e.g., *Benedetti et al.*, 2003] hypothesized in the central sector from geomorphology and subsurface geology (Figures 4 and 6). In this region few active faults are recognized (Figure 6), both because of the small size of the earthquakes (*M* is generally <6) and because of their depth (>10 km). However, we hypothesize that 10–20 km deep thrust events of *M* 5–6 could occur along the outer front of the northern Apennines, from Piedmont to the Adriatic coast of the Marche region. Indeed, some "new" faults have been recently proposed by *Valensise and Pantosti* [2001], even if they are not associated to known earthquakes, as for instance along the coast of Marche and Romagna. The stress directions shown in the smoothed map suggest that these faults can be active as thrust faults (Figure 6). This compressional regime with $S_{h\min}$ directions rotating from approximately E-W in the Po Plain to NW-SE along the Adriatic coast, follows the main tectonic structures of the Pleistocene age (Figure 4). This is probably related to a still active compression due to trench retreat of the northern Apennines [*Malinverno and Ryan*, 1986] and to the possible residual subduction beneath it [*Selvaggi and Amato*, 1992; *Amato and Cimini*, 2001; *Piromallo and Morelli*, 2003].

[32] As already described in previous studies, the internal sector of the northern Apennines is undergoing NE extension (Figure 3), as well evident from several recent earthquakes (Umbria-Marche 1997 and 1998; Norcia 1979; Gubbio 1984). It seems that the NE-SW extension affects the whole "back arc" region [see also *Frepoli and Amato*, 1997; *Montone et al.*, 1997; *Mariucci et al.*, 1999a], although most of the seismic deformation is released along the belt. Stress data in the Tyrrhenian coastal region (Figure 3) show a continuity in this process of extension that, as evidenced by geological data, started in the west and migrated to the east in the past 10–12 Myr [*Sartori*, 1990; *Jolivet et al.*, 1998]. In this area no data on active faults exist [*Valensise and Pantosti*, 2001].

[33] The Dinarides, on the other side of the Adriatic, are undergoing compression perpendicular to the trend of the belt. *Anderson and Jackson* [1987] explained the contemporaneous extension in the southern Apennines and the compression in the Dinarides with the counterclockwise rotation of the Adriatic microplate. This kind of motion seems to be in agreement with recent GPS data [*Serpelloni et al.*, 2002], but on the contrary, paleomagnetic analyses from Plio-Pleistocene units, performed to test the geodynamical evolution of the whole Adriatic block, show that no rotation has occurred since Late Pliocene [*Meloni et al.*, 1997]. Adding also the active compression at the outer front of the Apennines, north of 43°N suggests that the active deformation around the Adriatic Sea cannot be related to a simple rotation. Moreover, our new data in the central Adriatic Sea (Figure 6) show a compression zone, as already supposed by other authors [*Argnani and Frugoni*, 1997], that could connect the Italian compressive structures to the Dinarides structures. At present, these data are the only source of information that provide some constraints on the active tectonics of this sector. No data exist in the other available maps.

[34] In the central southern Apennines the existence of a clear extension perpendicular to the axis of the belt is well known [see i.e., *Anderson and Jackson*, 1987; *Jackson and McKenzie*, 1988; *Patacca and Scandone*, 1989; *Westaway et al.*, 1989; *Pondrelli et al.*, 1995; *Amato and Montone*, 1997]. Most of the recent seismicity is concentrated in a 30 to 50 km wide belt along the Apennines, and so are most of the historical sources, which appear to be associated to NW-SE trending normal faults (Figure 6). The stress conditions of this sector are very well depicted by the smoothed map, which in this region is constrained by both fault plane solutions and breakouts which sample the whole seismogenic crust. Faults in this area are therefore expected to rupture with normal faulting mechanisms throughout the whole belt, at least in the most active central sector, with individual lengths up to 40–50 km, i.e., $M \approx 7$ events or greater, as suggested by historical data.

[35] The stress data also indicate that the NE-SW direction of $S_{h\min}$ continues toward the foredeep, possibly in a strike-slip stress regime, as suggested by *Amato and Montone* [1997]. Other data on the tectonic setting of Italy confirm the absence of active compression along the southern Apennines outer front [*Meletti et al.*, 2000]. The recent Molise earthquakes of October–November 2002 (S. Pondrelli et al., Fast determination of moment tensors for the recent Molise (southern Italy) seismic sequence, *ORFEUS Electronic Newsletter*, *5*(1), 2, 2003, available at http://orfeus.knmi.nl/newsletter/vol5no1/molise.html), as the 1990 and 1991 Potenza earthquakes, support this idea, emphasizing the existence of E-W right-lateral strike-slip faults dissecting the belt. As previously hypothesized, the direction of maximum horizontal extension remains rather constant from the belt to the Apulian foreland. The change we observe is therefore linked to the switching of σ_1 and σ_2, from the vertical to the horizontal, while σ_3 remains horizontal, trending NE-SW (Figure 6). Possible causes for this rotation are the bending of the Apulian plate beneath the foredeep or, alternatively, the existence of E-W oriented shear zones inherited from previous tectonics [*Finetti*, 1982; *Doglioni*, 1991; *Doglioni et al.*, 1994], which act as transfer faults under a normal faulting regime, accommodating zones along the Apulian margin that rotate or retreat at different speed. No seismogenic source has been yet recognized along the entire southern Apennines foredeep and Apulian foreland except for the Gargano region [*Valensise and Pantosti*, 2001].

[36] Going from the southern Apennines to the Calabrian arc, we observe a gradual rotation of the $S_{h\min}$ direction from NE-SW to NW-SE, following the curvature of the arc itself. The larger faults inferred in this region from intensity data [*Valensise and Pantosti*, 2001] are expected to rupture with normal faulting mechanisms striking along the chain, whereas those oriented perpendicular to the arc would be either strike-slip or transpressive features (Figure 6). Some evidence of active transpression is found in the Ionian offshore, where the Ionian lithosphere underthrusts Calabria. This is in agreement also with the small earthquakes

pattern in this area [*Frepoli et al.*, 1996]. This peculiar stress distribution is probably related to the still active subduction of the deep slab descending below the southern Tyrrhenian Sea [*Lucente et al.*, 1999; *Amato and Cimini*, 2001]. The down-dip compression of this narrow slab is continuous throughout all its length, from 100 down to 400 km and possibly deeper, suggesting a process of passive sinking in the mantle [*Selvaggi*, 2001].

[37] Active extension is evident as far south as the Messina strait (Figure 6), where a $M > 7$ earthquake devastated the region in 1908 [*Pino et al.*, 2000]. More uncertain are the stress data and faulting regime in eastern Sicily (Figure 6), where another devastating shock occurred in 1693 along the southern coast [*Boschi et al.*, 1997; also http://80.117.141.2/cft]. There is no consensus about which fault produced this earthquake: it is hypothesized either along the N-S trending Hyblean-Malta escarpment, along a NE-SW thrust fault separating the foreland from the foredeep of the Catania Plain, or along an approximately N-S strike-slip fault cutting the Hyblean region. Here the stress map is based on a few earthquakes and many borehole breakouts and the resulting stress regime is prevailing strike slip, at least offshore (Figure 6). However, on land, the $S_{h\min}$ stress directions rotate from ENE-WSW in the Hyblean foreland, consistently with the direction of Africa-Europe convergence [*De Mets et al.*, 1990; *Sella et al.*, 2002] to NNW-SSE in the foredeep, the region between southernmost Sicily and Mount Etna. This stress rotation, which resembles in some way that observed in the northern Apennines, may indicate the coexistence of two stress regimes at very short distance. Unfortunately, the absence of earthquakes in southernmost Sicily does not indicate the stress regime for all this region. Moving westward from the Messina Strait, the present seismicity shows that the deformation is today concentrated on a narrow belt offshore the northern Sicily coast, where several M 5–6 earthquakes occurred in the past 20 years. Most of these earthquakes have thrust mechanisms with a N-S compression. A nearly N-S motion in this region is also documented by GPS data [*Serpelloni et al.*, 2002; *Hollenstein et al.*, 2003]. This kind of deformation is more in agreement with the Europe-Africa convergence (Figure 6) rather than the extension of the Tyrrhenian Sea. The opening of this basin is recent and the extension probably still active [*Argnani and Savelli*, 1999; *Faccenna et al.*, 2001], following the rollback of the slab, only toward the southeasternmost part of the basin, where the trench can retreat because oceanic lithosphere is still present. The northward motion of Sicily prevails west of the Aeolian Islands, where the oceanic lithosphere is completely consumed, the retreat process and extension are terminated and the northward Africa push dominates. In spite of the absence of any active fault mapped here [*Valensise and Pantosti*, 2001], the stress distribution indicates that offshore the northern Sicily coast thrust or reverse faults are likely to activate in future. An interesting question arises about the seismicity inland Sicily. The only significant earthquake in historical and recent times occurred in 1968 in Belice (event 143 in Table 2), western Sicily, and had a reverse mechanism with a large strike-slip component [*Anderson and Jackson*, 1987]. Other earthquakes in historical times were hypothesized by *Guidoboni et al.* [2002], based on the destruction of the Greek temple of Selinunte, but this information does not identify any preferred fault nor it does rule out the occurrence of future earthquakes in the central and western Sicily. The stress data available here show $S_{h\min}$ directions trending WNW-ESE, but any attempt to predict which faults may be activated and with which mechanism is highly speculative (Figure 6).

6. Conclusions

[38] This work characterizes the active stress field in Italy using borehole stress measurements, earthquake focal mechanisms and kinematic indicators on faults, to deduce the orientation, the regime and the distribution of the stress in the continental crust. The understanding of active stress conditions in Italy is now supported by a much larger amount and better distribution of data, which allow characterization of the stress field in regions that previously were not sampled. Our results of the tectonic setting confirm some of the first-order features outlined by previous Authors [i.e., *Malinverno and Ryan*, 1986; *Anderson and Jackson*, 1987; *Patacca and Scandone*, 1989; *Westaway*, 1992], and allow to better constrain direction and stress regime of large part of the territory. In particular, the new data are significant along the northern Apennine front, from the Po Plain to the Adriatic offshore, and along the southern Tyrrhenian Sea, north of Sicily, pointing out a compressive tectonic regime approximately N-S oriented. In the Alps both compressive and strike-slip regimes are observed. Our data also confirm that the whole Apenninic belt and the Calabrian arc are extending. Along the central Adriatic coast changes from one stress regime to another are shown. Stress rotations not associated to a stress regime variation follow the curvature of the arcs, as for instance from the southern Apennines to the Calabrian arc.

[39] By smoothing an updated data set of stress orientations we draw the regional stress pattern of Italy and define its relationship with the main tectonic features of the area giving constraints to the construction of numerical models. With respect to the previously published interpolated stress map of the Italian region, proposed by *Rebaï et al.* [1992], our smoothed map benefits from the much greater number of data that 12 more years made available. The comparison among our smoothed map (Figure 5a), the data set (Figure 3), the tectonic setting (Figure 4) [*Meletti et al.*, 2000], and the database of potential sources [*Valensise and Pantosti*, 2001] allows us to assign a stress regime to most of the Italian region (Figure 6) and to infer the nature of fault mechanisms of future expected earthquakes.

[40] **Acknowledgments.** Part of this work has been carried out in the framework of GNDT Project "Probable earthquakes in Italy between year 2000 and 2030: guidelines for determining priorities in seismic risk mitigation". We are grateful to B. Müller for providing the software used for smoothing stress data and to O. Heidbach for his help with the code. ENI-AGIP is thanked for new borehole data and in particular M. Cesaro for his help to recover data. We also thank A. Malinverno, R. Westaway, and G. Spada for useful suggestions and criticism.

References

Amato, A., and G. B. Cimini (2001), Deep structures from seismic tomography, in *Anatomy of an Orogen: The Apennines and Adjacent Mediterranean Basins*, edited by G. B. Vai and I. P. Martini, pp. 33–46, Kluwer Acad., Norwell, Mass.

Amato, A., and P. Montone (1997), Present-day stress field and active tectonics in southern peninsular Italy, *Geophys. J. Int.*, *130*, 519–534.

Amato, A., P. Montone, and M. Cesaro (1995), State of stress in southern Italy from borehole breakout and focal mechanism data, *Geophys. Res. Lett.*, *22*, 3119–3122.

Anderson, E. M. (1951), *The Dynamics of Faulting*, 2nd ed., Oliver and Boyd, White Plains, N. Y.

Anderson, H., and J. Jackson (1987), Active tectonics of the Adriatic region, *Geophys. J. R. Astron. Soc.*, *91*, 937–987.

Angelier, J. (1984), Tectonic analysis of fault slip data set, *J. Geophys. Res.*, *89*, 5835–5848.

Argnani, A., and F. Frugoni (1997), Foreland deformation in the Central Adriatic and its bearing on the evolution of the northern Apennines, *Ann. Geofis.*, *40*(3), 771–780.

Argnani, A., and C. Savelli (1999), Cenozoic volcanism and tectonics in the southern Tyrrhenian sea: Space-time distribution and geodynamic significance, *J. Geodyn.*, *27*, 409–432.

Arvidsson, R., and G. Ekström (1998), Global CMT analysis of moderate earthquakes M_w = 4.5 using intermediate period surface waves, *Bull. Seismol. Soc. Am.*, *88*, 1003–1013.

Azzara, R., A. Amato, A. Basili, C. Chiarabba, G. B. Cimini, M. Cocco, M. Di Bona, S. Mazza, and G. Selvaggi (1993), A detailed seismological study of a shallow active fault in northern Sicily (Italy), *Eos Trans. AGU*, *74*(43), Fall Meet. Suppl., F417.

Bassi, G., R. Sabadini, and S. Rebaï (1997), Modern tectonic regime in the Tyrrhenian area: Observations and models, *Geophys. J. Int.*, *129*, 330–346.

Bell, J. S., and D. I. Gough (1983), The use of borehole breakouts in the study of crustal stress, in *Hydraulic Fracturing Stress Measurements*, edited by M. D. Zoback and B. C. Haimson, pp. 201–209, Natl. Acad. Press, Washington, D. C.

Benedetti, L., P. Tapponier, G. C. P. King, and L. Piccardi (1998), Surface rupture of the 1857 southern Italy earthquake, *Terra Nova*, *10*, 206–210.

Benedetti, L. C., P. Tapponier, Y. Gaudemar, I. Manighetti, and J. Van Der Woerd (2003), Geomorphic evidence for an emergent active thrust along the edge of the Po Plain: The Broni-Stradella fault, *J Geophys. Res.*, *108*(B5), 2238, doi:10.1029/2001JB001546.

Boncio, P., F. Brozzetti, and G. La Vecchia (1996), State of stress in the northern Umbria-Marche Apennines (central Italy): Inferences from microearthquake and fault kinematic analyses, *Ann. Tectonicae*, *10*, 80–97.

Boschi, E., E. Guidoboni, G. Ferrari, G. Valensise, and P. Gasperini (1997), *Catalog of Strong Italian Earthquakes From 461 B.C. to 1990*, 973 pp., Storia Geofis. Ambiente, Ist. Naz. di Geofis. e Vulcanol., Rome, Italy.

Bressan, G., P. L. Bragato, and C. Venturini (2003), Stress and strain tensors based on focal mechanisms in the seismotectonic framework of the Friuli-Venezia Giulia region (northeastern Italy), *Bull. Seismol. Soc. Am.*, *93*(3), 1280–1297.

Caccamo, D., G. Neri, A. Sarao, and M. Wyss (1996), Estimates of stress directions by inversion of earthquake fault-plane solutions in Sicily, *Geophys. J. Int.*, *125*, 857–868.

Cesaro, M. (1993), Plateau Ibleo: Campo di stress da studi di breakout, analisi e modello interpretativo, internal report, Agenzia Ital. Pet. (AGIP), San Donato Milanese, Italy.

Cinti, F. R., L. Cucci, D. Pantosti, G. D'Addezio, and M. Meghraoui (1997), A major seismogenic fault in a silent area: The Castrovillari fault (southern Apennines, Italy), *Geophys. J. Int.*, *130*, 595–605.

Cucci, L., and G. Valensise (1995), Drainage pattern characteristics for the investigation of active faulting in Italy, *Terra Abstr.*, *7*, 38.

Cucci, L., S. Pondrelli, A. Frepoli, M. T. Mariucci, and M. Moro (2004), Local patterns of stress field and seismogenic sources in the Pergola-Melandro Basin and the Agri Valley (southern Italy), *Geophys. J. Int.*, *156*, 575–583, doi:10.1111/j.1365-246X.2004. 02161.x.

D'Addezio, G., E. Masana, and D. Pantosti (2001), The Holocene paleoseismicity of the Aremogna-Cinque Miglia Fault (central Italy), *J. Seismol.*, *5*, 181–205.

De Mets, C., R. G. Gordon, D. F. Argus, and S. Stein (1990), Current plate motion, *Geophys. J. Int.*, *101*, 425–478.

Dewey, J. F., M. L. Helman, E. Turco, D. H. W. Hutron, and S. D. Knott (1989), Kinematics of western Mediterranean, in *Alpine Tectonics*, edited by M. P. Coward, D. Detrich, and R. G. Park, *Geol. Soc. Spec. Publ.*, *45*, 265–283.

Doglioni, C. (1991), A proposal of kinematic modelling for W-dipping subductions: Possible applications to the Tyrrhenian-Apennines system, *Terra Nova*, *3*, 423–434.

Doglioni, C., F. Monelli, and P. Pieri (1994), The Puglia uplift (SE Italy): An anomaly in the foreland of the Apenninic subduction due to the buckling of a thick continental lithosphere, *Tectonics*, *13*, 1309–1321.

Dziewonski, A. M., T. A. Chou, and J. H. Woodhouse (1981), Determination of earthquake source parameters from waveform data for studies of global and regional seismicity, *J. Geophys. Res.*, *86*, 2825–2852.

Dziewonski, A. M., A. Friedman, D. Giardini, and J. H. Woodhouse (1983), Global seismicity of 1982: Centroid moment tensor solutions for 308 earthquakes, *Phys. Earth Planet. Inter.*, *53*, 17–45.

Dziewonski, A. M., G. Ekström, and N. N. Maternovskaya (2000), Centroid-moment tensor solutions for October–December 1999, *Phys. Earth Planet. Inter.*, *121*, 205–221.

Ekström, G., A. Morelli, E. Boschi, and A. M. Dziewonski (1998), Moment tensor analysis of the central Italy earthquake sequence of September–October 1997, *Geophys. Res. Lett.*, *25*, 1971–1974.

Eva, E., S. Solarino, C. Eva, and G. Neri (1997), Stress tensor orientation derived from fault plane solutions in the southwestern Alps, *J. Geophys. Res.*, *102*, 8171–8185.

Faccenna, C., T. W. Becker, F. P. Lucente, L. Jolivet, and F. Rossetti (2001), History of subduction and back-arc extension in the central Mediterranean, *Geophys. J. Int.*, *145*, 809–820.

Finetti, I. (1982), Structure, stratigraphy and evolution of central Mediterranean, *Boll. Geof. Teor. Appl.*, *24*(96), 247–312.

Frepoli, A., and A. Amato (1997), Contemporaneous extension and compression in the northern Apennines from earthquake fault-plane solutions, *Geophys. J. Int.*, *129*, 368–388.

Frepoli, A., and A. Amato (2000a), Spatial variation in stresses in peninsular Italy and Sicily from background seismicity, *Tectonophysics*, *317*(1–2), 109–124.

Frepoli, A., and A. Amato (2000b), Fault plane solutions of crustal earthquakes in southern Italy (1988–1995), Seismotectonic implications, *Ann. Geofis.*, *43*, 437–467.

Frepoli, A., G. Selvaggi, C. Chiarabba, and A. Amato (1996), State of stress in the southern Tyrrhenian subduction zone from fault-plane solutions, *Geophys. J. Int.*, *125*, 879–891.

Galli, P., and V. Bosi (2002), Paleoseismology along the Cittanova fault: Implications for seismotectonics and earthquake recurrence in Calabria (southern Italy), *J. Geophys. Res.*, *107*(B3), 2044, doi:10.1029/2001JB000234.

Gasparini, C., G. Iannaccone, and R. Scarpa (1985), Fault-plane solutions and seismicity of the Italian peninsula, *Tectonophysics*, *117*, 59–78.

Guidoboni, E., A. Muggia, C. Marconi, and E. Boschi (2002), An archaeoseismology's research: The collapses of the temples at Selinunte (southwestern Sicily), *Bull. Seismol. Soc. Am.*, *92*(8), 2961–2982.

Hansen, K. M., and V. S. Mount (1990), Smoothing and extrapolation of crustal stress orientation measurements, *J. Geophys. Res.*, *95*, 11,805–11,820.

Hollenstein, C., H. G. Kahle, A. Geiger, S. Jenny, S. Goes, and D. Giardini (2003), New GPS constraints of the Africa-Eurasia plate boundary zone in southern Italy, *Geophys. Res. Lett.*, *30*(18), 1935, doi:10.1029/2003GL017554.

Hüsges, S. (1995), Modellierung der tektonischen Spannungen der Eurasischen Platte. M.S. thesis, Univ. of Karlsruhe, Karlsruhe, Germany.

Jackson, J., and D. McKenzie (1988), The relationship between plate motions and seismic moment tensors, and the rate of active deformation in the Mediterranean and Middle East, *Geophys. J.*, *93*, 45–73.

Jolivet, L., et al. (1998), Midcrustal shear zones in postorogenic extension: Example from the northern Tyrrhenian Sea, *J. Geophys. Res.*, *103*, 12,123–12,160.

Lucente, F. P., C. Chiarabba, G. B. Cimini, and D. Giardini (1999), Tomographic constraints on the geodynamic evolution of the Italian Region, *J. Geophys. Res.*, *104*, 20,307–20,327.

Malinverno, A., and W. B. F. Ryan (1986), Extension in the Tyrrhenian Sea and shortening in the Apennines as a result of arc migration driven by sinking of the lithosphere, *Tectonics*, *5*, 227–245.

Mariucci, M. T., and B. Müller (2003), The tectonic regime in Italy inferred from borehole breakout data, *Tectonophysics*, *361*, 21–35.

Mariucci, M. T., A. Amato, and P. Montone (1999a), Recent tectonic evolution and present stress in the northern Apennines, *Tectonics*, *18*, 108–118.

Mariucci, M. T., A. Amato, and P. Montone (1999b), New breakout data in northern Italy, paper presented at the 2nd World Stress Map Euroconference on Deformation and stress in the Earth's Crust, Aspo, Sweden, 22–26 Sept.

Mariucci, M. T., A. Amato, R. Gambini, M. Giorgioni, and P. Montone (2002), Along-depth stress rotations and active faults: An example in a 5-km deep well of southern Italy, *Tectonics*, *21*(4), 1021, doi:10.1029/2001TC001338.

McGarr, A., and N. C. Gay (1978), State of stress in the Earth's crust, *Annu. Rev. Earth Planet. Sci.*, *6*, 405–436.

McKenzie, D. P. (1969), The relation between fault plane solutions for earthquakes and the directions of the principal stress, *Bull. Seismol. Soc. Am.*, *59*, 591–601.

Meletti, C., E. Patacca, and P. Scandone (2000), Construction of a seismotectonic model: The case of Italy, *Pure Appl. Geophys.*, *157*, 11–35.

Meloni, A., L. Alfonsi, F. Florindo, L. Sagnotti, F. Speranza, and A. Winkler (1997), Neogene and Quaternary geodynamic evolution of the Italian peninsula: The contribution of paleomagnetic data, *Ann. Geofis.*, *40*(3), 705–727.

Michael, A. J. (1987), The use of focal mechanisms to determine stress: A control study, *J. Geophys. Res.*, *92*, 357–368.

Michetti, A. M., L. Ferreli, L. Serva, and E. Vittori (1997), Geological evidence for strong historical earthquakes in an aseismic region: The Pollino case (southern Italy), *J. Geodyn.*, *24*, 67–86.

Montone, P., and M. T. Mariucci (1999), Active stress along the NE external margin of the Apennines: The Ferrara arc, northern Italy, *J. Geodyn.*, *28*, 251–265.

Montone, P., A. Amato, R. Chiulli, and R. Funiciello (1992), Metodologie per la determinazione del campo di stress attuale da dati di perforazioni profonde, paper presented at the 11th Meeting of Gruppo Nazionale di Geofisica della Terra Solida, Cons. Naz. delle Ric., Rome, Italy.

Montone, P., A. Amato, C. Chiarabba, G. Buonasorte, and A. Fiordelisi (1995), Evidence of active extension in Quaternary volcanoes of central Italy from breakout analysis and seismicity, *Geophys. Res. Lett.*, *22*, 1909–1912.

Montone, P., A. Amato, A. Frepoli, M. T. Mariucci, and M. Cesaro (1997), Crustal stress regime in Italy, *Ann. Geofis.*, *40*, 741–757.

Montone, P., A. Amato, and S. Pondrelli (1999), Active stress map of Italy, *J. Geophys. Res.*, *104*, 25,595–25,610.

Müller, B., V. Wehrle, S. Hettel, B. Sperner, and K. Fuchs (2003), A new method for smoothing orientated data and its application to stress data, in *Fracture and In-Situ Stress Characterization of Hydrocarbon Reservoirs*, edited by M. S. Ameen, *Geol. Soc. Spec. Publ.*, *209*, 107–126.

Pantosti, D., G. D'Addezio, and F. R. Cinti (1996), Paleoseismicity of the Ovindoli-Pezza fault, central Apennines, Italy: A history including a large, previously unrecorded earthquake in the Middle Ages (860–1300 A.D.), *J. Geophys. Res.*, *101*, 5937–5959.

Patacca, E., and P. Scandone (1989), Post-Tortonian mountain building in the Apennines. The role of passive sinking of a relic lithospheric slab, in *The Lithosphere in Italy: Advances in Earth Science Research*, edited by Boriani et al., pp. 157–176, Accad. Naz. Dei Lincei, Rome, Italy.

Pino, N. A., D. Giardini, and E. Boschi (2000), The 1908 December 28 Messina Straits, southern Italy, earthquake: Waveform modelling of regional seismograms, *J. Geophys. Res.*, *105*, 25,473–25,492.

Piromallo, C., and A. Morelli (2003), P wave tomography of the mantle under the Alpine-Mediterranean area, *J. Geophys. Res*, *108*(B2), 2065, doi:10.1029/2002JB001757.

Pondrelli, S., A. Morelli, and E. Boschi (1995), Seismic deformation in the Mediterranean area estimated by moment tensor summation, *Geophys. J. Int.*, *122*, 938–952.

Pondrelli, S., A. Morelli, and G. Ekstrom (1998), Moment tensors and seismotectonics of the Mediterranean region, *Ann. Geophys.*, *16*, suppl., C19.

Pondrelli, S., G. Ekström, A. Morelli, and S. Primerano (1999), Study of source geometry for tsunamigenic events of the Euro-Mediterranean area, in *International Conference on Tsunamis*, pp. 297–307, UNESCO Books, Paris.

Pondrelli, S., G. Ekström, and A. Morelli (2001), Seismotectonic re-evaluation of the 1976 Friuli, Italy, seismic sequence, *J. Seismol.*, *5*, 73–83.

Pondrelli, S., A. Morelli, G. Ekström, S. Mazza, E. Boschi, and A. M. Dziewonski (2002), European-Mediterranean regional centroid-moment tensors: 1997–2000, *Phys. Earth Planet. Inter.*, *130*, 71–101.

Ragg, S., M. Grasso, and B. Müller (1999), Patterns of tectonic stress in Sicily from borehole breakout observations and finite element modelling, *Tectonics*, *18*, 669–685.

Rebaï, S., H. Philip, and A. Taboada (1992), Modern tectonics stress field in the Mediterranean region: Evidence for variation in stress directions at different scales, *Geophys. J. Int.*, *110*, 106–140.

Sartori, R. (1990), The main results of ODP Leg 107 in the frame of Neogene to Recent geology of peri-Tyrrhenian areas, *Proc. Ocean Drill. Program Sci. Results*, *107*, 715–730.

Sella, G. F., T. H. Dixon, and A. Mao (2002), REVEL: A model for Recent plate velocities from space geodesy, *J. Geophys. Res.*, *107*(B4), 2081, doi:10.1029/2000JB000033.

Selvaggi, G. (2001), Strain pattern of the southern Tyrrhenian slab from moment tensors of deep earthquakes: Implications on the down-dip velocity, *Ann. Geofis.*, *44*, 155–165.

Selvaggi, G., and A. Amato (1992), Subcrustal earthquakes in the northern Apennines (Italy): Evidence for a still active subduction?, *Geophys. Res. Lett.*, *19*, 2127–2130.

Selvaggi, G., and C. Chiarabba (1995), Seismicity and P-wave velocity image of the southern Tyrrhenian subduction zone, *Geophys. J. Int.*, *122*, 818–826.

Selvaggi, G., B. Castello, and R. Azzara (1997), Spatial distribution of scalar seismic moment release in Italy (1983–1996): Seismotectonic implications for the Apennines, *Ann. Geofis.*, *40*, 1565–1578.

Selvaggi, G., et al. (2001), The M_w 5.4 Reggio Emilia 1996 earthquake: Active compressional tectonics in the Po Plain, Italy, *Geophys. J. Int.*, *144*, 1–13.

Serpelloni, E., M. Anzidei, P. Baldi, G. Casula, A. Galvani, A. Pesci, and F. Riguzzi (2002), Combination of permanent and non-permanent GPS networks for the evaluation of the strain-rate field in the central Mediterranean area, *Boll. Geofis. Teor. Appl.*, *43*, 195–219.

Valensise, G., and D. Pantosti (Eds.) (2001), Database of potential sources for earthquakes larger than *M* 5. 5 in Italy [CD-ROM], *Ann. Geofis.*, *44* (4), suppl., 180 pp.

Ward, S. N., and G. Valensise (1989), Fault parameters and slip distribution of the 1915, Avezzano, Italy earthquake derived from geodetic observations, *Bull. Seismol. Soc. Am.*, *79*, 690–710.

Watson, G. S. (1985), Interpolation and smoothing of directed and undirected line data, in *Multivariate Analysis-VI*, edited by P. R. Krishnajah, pp. 613–625, Elsevier Sci., New York.

Wehrle, V. (1998), Analytische Untersuchung intralithosphärischer Deformationen und Numerische Bestimmung krustaler Spannungsdomänen, Ph.D. thesis, 167 pp., Univ. of Karlsruhe, Karlsruhe, Germany.

Westaway, R. (1987), The Campania, southern Italy, earthquakes of 1962 August 21, *Geophys. J. R. Astron. Soc.*, *88*, 1–24.

Westaway, R. (1992), Seismic moment summation for historical earthquakes in Italy: Tectonic implications, *J. Geophys. Res.*, *97*, 15,437–15,464.

Westaway, R. (1993), Quaternary uplift of southern Italy, *J. Geophys. Res.*, *98*, 21,741–21,772.

Westaway, R., R. Gawthorpe, and M. Tozzi (1989), Seismological and field observations of the 1984 Lazio-Abruzzo earthquakes: Implications for the active tectonics of Italy, *Geophys. J. R. Astron. Soc.*, *98*, 489–514.

Zoback, M. L. (1992), First- and second-order patterns of stress in the lithosphere: The World Stress Map Project, *J. Geophys. Res.*, *97*, 11,703–11,728.

A. Amato, M. T. Mariucci, P. Montone, and S. Pondrelli, Istituto Nazionale di Geofisica e Vulcanologia, Via di Vigna Murata 605, I-00143, Italy. (montone@ingv.it)